Revision Number: YCLNU-D-20-01565

Zinc deficiency leads to reduced interleukin-2 production by active gene silencing due to enhanced CREMα expression in T cells

Short title: Zinc deficiency leads to IL-2 gene silencing

Authors:

Veronika Kloubert [a], Inga Wessels [a], Jana Wolf [a], Karoline Blaabjerg [b], Veerle Janssens [c], Jan Hapala [d,e], Wolfgang Wagner [d,e], Lothar Rink [a,*]

Affiliations:

[a] Institute of Immunology, Faculty of Medicine, RWTH Aachen University, Pauwelsstr. 30, 52074 Aachen, Germany.

[b] Department of Animal Science – Animal Nutrition and Physiology, Aarhus University/Foulum, Blichers Allé 20, 8830 Tjele, Denmark.

[c] Laboratory of Protein Phosphorylation & Proteomics, Department of Cellular and Molecular Medicine, Faculty of Medicine, KU Leuven & LKI (Leuven Cancer Institute, KU Leuven), Leuven, Belgium.

[d] Helmholtz Institute for Biomedical Engineering, Stem Cell Biology and Cellular Engineering, RWTH Aachen University, Pauwelsstr. 20, 52074 Aachen, Germany.

[e] Institute of Biomedical Engineering, Department of Cell Biology, Faculty of Medicine, RWTH Aachen University, Pauwelsstr. 30, 52074 Aachen.

[*] Corresponding author. Email: LRink@ukaachen.de

Abstract

Background & Aims:

The micronutrient zinc is essential for proper immune function. Consequently, zinc deficiency leads to impaired immune function, as seen in decreased secretion of interleukin (IL)-2 by T cells. Although this association has been known since the late 1980s, the underlying molecular mechanisms are still unknown. Zinc deficiency and reduced IL-2 levels are especially found in the elderly, which in turn are prone to chronic diseases. Here, we describe a new molecular link between zinc deficiency and reduced IL-2 expression in T cells.

Methods:

The effects of zinc deficiency were first investigated *in vitro* in the human T cell lines Jurkat and Hut-78 and complemented by *in vivo* data from zinc-supplemented pigs. A short- and long-term model for zinc deficiency was established. Zinc levels were detected by flow cytometry and expression profiles were investigated on the mRNA and protein level.

Results:

The expression of the transcription factor cAMP-responsive-element modulator α (CREMα) is increased during zinc deficiency *in vitro*, due to increased protein phosphatase 2A (PP2A) activity, resulting in decreased IL-2 production. Additionally, zinc supplementation *in vivo* reduced CREMα levels causing increased IL-2 expression. On epigenetic levels increased CREMα binding to the IL-2 promoter is mediated by histone deacetylase 1 (HDAC1). The HDAC1 activity is inhibited by zinc. Moreover, deacetylation of the activating histone mark H3K9 was increased under zinc deficiency, resulting in reduced IL-2 expression.

Conclusions:

With the transcription factor CREMα a molecular link was uncovered, connecting zinc deficiency with reduced IL-2 production due to enhanced PP2A and HDAC1 activity.

Keywords

Zinc deficiency, interleukin-2, CREM alpha, Histone deacetylase, T cells

Introduction

Interleukin (IL)-2 is a cytokine produced by activated T cells and is essential for their proliferation and survival. Furthermore, IL-2 contributes to the activity of cytolytic natural killer cells and is important for the generation and function of regulatory T cells, thus ensuring proper immune functions [1]. IL-2-induced pathways influence gene expression by regulating apoptosis, cellular growth and immune functions [2]. Various transcription factors are involved in the regulation of IL-2 transcription, such as nuclear factor κ-light-chain-enhancer of activated B cells (NF-κB) and CREMα [1]. By alternative splicing several CREM isoforms originate, encoding for activators on the one hand, such as CREMτ, and encoding for repressors on the other hand, such as CREMα [3]. Impaired IL-2 expression is associated with immunological dysfunctions, as seen in systemic lupus erythematosus (SLE) and is moreover associated to increased CREMα expression in T cells of SLE patients [4]. Those patients have lower serum zinc levels compared to healthy control subjects [5–7]. CREMα binds to the -180 cAMP responsive element (CRE) site within the IL-2 promoter, thereby inhibiting IL-2 transcription and increasing the patients' susceptibility to infections [8,9]. This CRE site is localized within a minimal enhancer region upstream of the transcription initiation site of the *IL2* gene which comprises approx. 300 bp. Apart from that CRE site, the enhancer region harbors binding sites for other regulatory elements, as for example binding sites for activator protein-1 or NF-κB [1]. The expression of the transcription factor CREMα itself is further regulated by the transcription factor "specificity protein 1" (SP-1). The protein phosphatase 2A (PP2A) activates SP-1 causing the transcription of CREMa, which among others represses the expression of IL-2 [10].

Nutritional deficiencies, such as zinc deficiency, negatively influence the immune system, as seen in reduced IL-2 production by T cells, which is reported since the late 1980s [11–14]. Furthermore, mild zinc deficiency is associated with decreased thymulin activity and a reduced $CD4^+/CD8^+$

T cell ratio [13]. The essential trace element zinc is needed for growth and development of all organisms. It is important for the function of more than 300 enzymes, covering all enzyme classes. The need of zinc in proliferation processes, DNA and RNA synthesis, and apoptosis-related pathways emphasizes moreover its importance in biological processes [15]. The total zinc amount within the human body comprises 2-4 g. However, the plasma zinc concentration is low with only 12-16 µM zinc, which highlights the importance of steady state zinc intake. Otherwise, zinc deficiency could develop since there is no zinc storage system within the human body [14]. Regulation of zinc homeostasis is thus very important and needs to be ensured, as for example by zinc transporters. Two families of zinc transporters exist, comprising the Zip (Zrt-, Irt-like protein)/SLC39A (solute carrier family 39) and ZnT (zinc transporter)/SLC30A families with 14 importers and 10 exporters, respectively [16]. Additionally, the metal-response element-binding transcription factor (MTF)-1 is a cellular zinc ion sensor which regulates the transcription of genes containing metal-response elements (MRE) in their promotor [17].

Several studies reported already an association of zinc with altered IL-2 expression. *In vitro* zinc resupplementation of zinc-deficient murine EL-4 6.1 T cells, beneficially increased IL-1β-induced IL-2 expression [18]. Besides, zinc supplementation of zinc-deficient elderly increased the amount of IL-2 mRNA produced by isolated mononuclear cells, going along with decreased incidence of infections [19]. However, not only elderly showed an improved immune status after zinc supplementation, but also in zinc-deficient patients suffering from sickle cell disease, zinc supplementation improved the IL-2 expression by stimulated peripheral blood mononuclear cells (PBMC), being accompanied by reduced incidence of infections, as well [20].

However, the molecular mechanisms studied so far, do not completely explain the altered IL-2 production under zinc-deficient conditions. Therefore, the analysis of zinc effects on epigenetic mechanisms, influencing IL-2 expression in T cells, might be an interesting new approach. The

aim of this study was to elucidate new molecular targets which are affected by zinc, thus leading to decreased IL-2 expression.

Materials and Methods

Study Design

The aim of this study was to elucidate new molecular targets which cause a decreased IL-2 expression in zinc-deficient conditions. For this purpose, a short- and long-term model for zinc deficiency was established. The effects of zinc deficiency were firstly investigated *in vitro* in human T cell lines and complemented by animal *in vivo* data. Flow cytometry, ELISA, qPCR, and Western blotting were used for analysis. Experiments were conducted in at least three independent replicates. Cell viability was monitored by propidium iodide staining whereby replicates with more than 26 % dead cells in total were excluded from the study.

Ethics statement

Research on porcine serum and PBMC was conducted according to license obtained from the Danish Animal Experiments Inspectorate, Ministry of Food, Agriculture and Fisheries, Danish Veterinary and Food Administration. The corresponding protocols were approved on June 3, 2013 and made public in anonymized form. This study was in compliance with the guidelines concerning animal experiments and care of animals under study, according to the Danish Ministry of Justice, Act. 726 of September 9, 1993, and as amended in Act. 1306 of November 23, 2007, which complies with the EU Directive 2010/63/EU for animal experiments.

Animals and diets

This study included 18 pigs (3 litters of 6 pigs each). The pigs were crossbred (Duroc x Danish Landrace x Yorkshire) females and castrated males and were housed individually in pens with ad

libitum access to food and water until the time of euthanasia. One batch of basal diet was prepared according to Danish recommendations for all nutrients for pigs between 6 and 9 kg except for zinc[21]. The pigs were given a basal diet for 1-2 weeks, supplemented with either 0 ppm, 100 ppm or 2500 ppm zinc from ZnO (Zn0, Zn100 and Zn2500, respectively). Without zinc supplementation the basal diet contained 59 ppm zinc due to the ingredients. The composition of the diet and the zinc treatment were previously described[22].

Isolation of PBMC

Porcine PBMC were isolated from sodium-heparinized whole blood samples (BD Vacutainer, Denmark). Blood was diluted in a ratio of 1:3 with PBS (Sigma-Aldrich, Germany). After density centrifugation over Biocoll separating solution with a density of 1.077 g/mL (Biochrom, Germany), cells were collected from the interface and washed with PBS. Subsequently, erythrocytes were lysed with water and remaining PBMC were washed again with PBS. Cells were resuspended in RPMI 1640 medium (Sigma-Aldrich, Germany) supplemented with 10 % heat-inactivated fetal calf serum (FCS) (PAA, Germany), 2 mM L-glutamine, 100 U/mL potassium penicillin and 100 U/mL streptomycin sulfate (all from Sigma-Aldrich, Germany). Viable cells were counted with trypan blue staining (Sigma-Aldrich, Germany) and adjusted to the concentration needed for the specific assays.

Inductively coupled plasma-mass spectrometry (ICP-MS)

Serum zinc levels were analyzed in blood collected from the jugular vein of the pigs (BD Vactuainer, Denmark) using ICP-MS. Zinc concentrations were analyzed on a X series II ICP-MS equipped with a conventional Meinhard nebulizer and a Peltier cooled quartz impact bead spray chamber operated at 3°C (Thermo Electron Corporation, Germany) set with a CETAC autosampler model ASX-520 (Thermo Fisher Scientific, USA). Data were collected using the PlasmaLab

version 2.5.9.30 (Thermo Electron Corporation, Germany). The instrument settings comprised 1400 W forward power, 13 L/min plasma gas (Ar), 0.9 L/min nebulizer gas (Ar) and 0.7 L/min auxiliary gas. The sample uptake comprised approx. 0.4 mL/min and ^{45}Sc, ^{71}Ga and ^{103}Rh were used as internal standards with interpolation.

Cell culture and zinc deficiency models

The human T cell lines HuT-78 and Jurkat were cultivated at 37°C in a humidified 5 % CO_2 atmosphere. Cells were seeded in RPMI 1640, containing 10 % heat-inactivated FCS, 2 mM L-glutamine, 100 U/mL potassium penicillin and 100 U/mL streptomycin sulfate for culture of HuT-78 T cells and additionally supplemented with 1 % 100x non-essential amino acids and 100 mM sodium pyruvate (all Sigma-Aldrich, Germany) for cultivation of Jurkat T cells.

To induce short-term zinc deficiency, HuT-78 and Jurkat T cells were cultured in medium containing the zinc chelator N,N,N',N'-tetrakis-(2-pyridyl-methyl)-ethylenediamine (TPEN) (Sigma-Aldrich, Germany) with a final concentration of 3 µM for three days. The TPEN concentration of 3 µM showed no toxic effects on HuT-78 (Fig. S1 A) and Jurkat T cells (Fig. S1 B), which was determined by cell viability measurements using propidium iodide (PI, Sigma-Aldrich, Germany).

To induce long-term zinc deficiency in Jurkat T cells for three weeks, culture medium was treated with the divalent cation chelating resin Chelex 100 (Sigma-Aldrich, Germany), which removes zinc from the medium. The chelated medium was reconstituted with 500 µM CaCl2, 400 µM MgCl2 [23,24] and 50 µg/L (0.174 µM) $ZnSO_4$, i.e. 25 % of the normal concentration in the medium (all from Merck, Germany). Additionally, the pH was adjusted to 7.4, resembling the pH value of the control medium. Replicates with more than 26 % dead cells in total were excluded from the study. Gated, structurally normal cells cultured in Chelex-treated medium showed no

significantly more dead cells than cells in control medium, which was determined by PI measurements (Fig. S1 C).

Flow cytometric measurement of intracellular free Zn^{2+} with FluoZin-3 AM and Zinpyr-1

HuT-78 and Jurkat T cells were incubated as described before in either control or zinc-deficient culture medium for short-term (HuT-78 and Jurkat) and long-term (Jurkat) analyses. $1x10^6$ cells per sample were loaded with 1 mL measurement buffer [25] for 30 min either with 1 µM FluoZin-3 AM (Thermo Fisher, Germany) or 10 µM Zinpyr-1 (Neurobiotex, USA), gently shaken at 37°C in the dark. Afterwards, cells were washed and resuspended in measurement buffer and samples were incubated for further 10 min at 37°C with either TPEN (50 µM) to obtain minimal fluorescence, with $ZnSO_4$/pyrithione (100 µM/50 µM) (all Sigma-Aldrich, Germany) to obtain maximal fluorescence, or were left untreated. Subsequent flow cytometry measurements were performed using FACSCalibur (BD, Germany) and gated, structurally normal cells were selected for analyses. Calculation of intracellular labile zinc was performed as described before [26] using the dissociation constant K_D of 8.9 nM for the FluoZin-3/Zn2+ complex [27] and KD of 0.7 nM for the Zinpyr-1/Zn2+ complex [28].

Flame atomic absorption spectrophotometry (AAS)

Zinc adequate control medium and Chelex-treated zinc-deficient medium for Jurkat T cells were analyzed by AAS (Analyst 800, Perkin Elmer, Germany). Measurement of total cell zinc concentrations was as well performed by AAS. $2x10^6$ cells were washed with wash buffer (0.9 % sodium chloride [NaCl, AppliChem, Germany], 10 mM ethylenediaminetetraacetic acid [EDTA, Sigma-Aldrich, Germany] and 10 mM N-[2-Hydroxyethyl]piperazine-N'-[2-ethanesulfonic acid] [HEPES, AppliChem, Germany]) and the pellet was afterwards resuspended in water. Cells were hydrolyzed in 200 µL HNO_3 for 2 h at 80°C followed by subsequent zinc measurements with AAS.

IL-2 quantification

Supernatants for IL-2 determination *in vitro* and *in vivo* were harvested from $1x10^6$ cells/mL. After induction of zinc deficiency for either three days or three weeks or after isolation of porcine PBMC, cells were stimulated for 24 h with 0.1 µM Cal/A23187 (Sigma-Aldrich, Germany) in combination with 10 ng/mL phorbol-12-myristate-13-acetate (PMA, Sigma-Aldrich, Germany) to induce T cell activation via direct protein kinase C activation. Additionally, samples were stimulated with 2.5 µg/mL phytohemagglutinin (PHA, Biochrom, Germany) for an alternative T cell activation via surface receptors, determining IL-2 in the supernatants of long-term and siRNA-transfected samples. Furthermore, these two stimulants were shown to behave differently regarding zinc signals [25]. Subsequently, supernatants were stored at -20°C. IL-2 protein concentrations in supernatants of HuT-78 and Jurkat T cells were determined by OptEIA ELISA assay (BD, Germany) according to the manufacturer's instructions with a detection limit of 7.8 pg/mL. Only the incubation steps were adjusted to 2 h incubation of standard and samples, 2 h incubation with the IL-2 detection antibody, 20 min incubation with streptavidin-horse radish peroxidase (HRP) conjugate and subsequent substrate solution incubation. IL-2 concentration in supernatants of porcine PBMC was determined by Swine IL-2 CytoSet ELISA (Invitrogen, USA) according to the manufacturer's instructions with a detection limit of 8.9 pg/mL. Here, the incubation steps were as well adjusted as described for the human IL-2 ELISA. Samples were measured by using Sunrise or Spark microplate reader (Tecan, Germany).

Quantitative real-time polymerase chain reaction (qPCR)

After short-term zinc deficiency, cells were left unstimulated as control or were stimulated with 1 µM Cal combined with 10 ng/mL PMA for 6 h to analyze CREMα expression. To analyze the CREMα and IL-2 expression after long-term zinc deficiency, cells were either left unstimulated,

stimulated with 2.5 µg/mL PHA or were stimulated with 0.1 µM Cal combined with 10 ng/mL PMA for 6 h and 24 h. RNA isolation and cDNA synthesis were performed, according to the manufacturer's instructions, using the NucleoSpin RNA II kit (Macherey-Nagel, Germany) and the qScript cDNA synthesis kit (VWR/QuantaBioscience, Germany), respectively. Quantitative analysis was performed using the fluorescent SYBR green reagent on a StepOnePlus Real-Time PCR System (Applied Biosystems, Germany) at 95°C for 10 min, followed by 40 cycles at 95°C for 15 sec and the indicated annealing temperature for 30 sec. The following primers were used: IL-2 [29] (58°C); CREMα [10], MTF-1 [30], porphobilinogen deaminase (PBGD) [31], Zip1 (forward primer: GCC TGA CTA CCT GGC TGC CAT AGA, reverse primer: CGG CCC TGA CTG CTC CTT GTA A), Zip2 (forward primer: GTG CAG AAC AGA TCA GCA AGT GA, reverse primer: CAA TGC CAG CGA CTC CAA A), Zip3 [32], Zip4-Zip12 [33], Zip14 [33], ZnT1-ZnT9 [34] (all 60°C); HDAC1 [35] (61°C); Zip13 [33] (62°C); ZnT10 (forward primer: CAC CCA GAA TGA GCC AGA AGA C, reverse primer: GAT AAG CGG GAA GGC AGA TGA C) (65°C).

Target gene expression was normalized to expression of the housekeeping gene PBGD. All samples were run in duplicates. Gene expression was quantified by use of the $\Delta\Delta C_T$-method as described before [36].

siRNA transfection

Knockdown of MTF-1 was performed using "Stealth siRNA MTF-1" and "Silencer Select negative control No. 1" siRNA was used as a negative control (both from Thermo Fisher, Germany), according to the manufacturer's instructions. Cells were seeded with $3x10^5$ cells/mL one day before transfection to ensure exponential cell growth. The next day, cells were harvested and resuspended in the above mentioned RPMI 1640 Jurkat medium, containing 20 % FCS and lacking antibiotics. Subsequently, $2.5x10^6$ cells per sample were transfected by electroporation

with 100 nM of the respective siRNA with a BioRad Gene Pulser II (Biorad, Germany) and 100 U/mL potassium penicillin and 100 U/mL streptomycin sulfate were added 4-6 h after electroporation. 24 h post-transfection, cells were stimulated for another 24 h with either 2.5 µg/mL PHA, 10 ng/mL PMA in combination with 0.1 µM Cal or left untreated as control. After stimulation, RNA isolation and cDNA synthesis were performed as described before to confirm MTF-1 silencing. Supernatants were collected for IL-2 quantification by OptEIA ELISA assay as described before.

DNA isolation and methylation analysis

DNA of $3x10^6$ Jurkat T cells was isolated after three weeks of incubation in either normal or Chelex-treated zinc-deficient medium by use of the QIAamp DNA Mini Kit, according to the manufacturer's instructions (Qiagen, Germany). Subsequent analysis of the DNA methylation pattern was performed on an EPIC BeadChip Microarray as costumized support by Life & Brain Center, Bonn.

Western Blot

Analysis of the following antibodies: phospho-Ser/Thr PKA substrate ($RRXS^*/T^*$), β-actin, c-Fos (9F6), acetyl-histone H3 (K9), acetyl-histone H3 (K18), phospho-histone H3 (S10), histone H3, phospho-NF-kappaBp65 (S276), phospho-p44/42 MAPK (T202/Y204), p44/42 MAPK (Erk1/2) (all from Cell Signaling Technology, Germany) and CREM C-2 (Santa Cruz Biotechnology, Germany).

$1x10^6$ Jurkat T cells, previously cultivated for three weeks in either control or Chelex-treated zinc-deficient medium, were either immediately prepared for Western Blot analysis or were seeded in a 24 well plate and stimulated with PMA/Cal (10 ng/mL/0.1 µM) for 6 h and 24 h or left untreated as control. Afterwards, cells were collected, centrifuged and resuspended in 100 µL sampling

buffer (65 mM Tris-HCl [pH 6.8], 2 % [w/v] SDS, 1 mM sodium orthovanadate, 26 % [v/v] glycerol, 1 % [v/v] β-mercaptoethanol and 0.01 % [w/v] bromphenol blue). For porcine CREMα detection, $2x10^6$ porcine PBMC were resuspended in sampling buffer. Cells were lysed by sonication using a Vibra Cell sonicator (Sonics & Materials, USA) and heated for 5 min at 95°C. An equivalent of $2x10^5$ cells or $4x10^5$ porcine PBMC per lane was separated at 170 V on 10 % polyacrylamide gels for the analysis of all used antibodies, except for analyses with acetyl-histone H3 (K9), acetyl-histone H3 (K18), phospho-histone H3 (S10), histone H3 and CREM C-2 antibodies, which were run on 15 % polyacrylamide gels. Samples run on 10 % gels and samples run on 15 % gels were blotted onto nitrocellulose membranes with 0.45 µM pore size or with 0.2 µM pore size (GE Healthcare Life Sciences, Germany), respectively. Uniform loading of gels was confirmed by Ponceau S (AppliChem, Germany) staining. Membranes were blocked for 1 h with TBS-T (20 mM Tris [pH 7.6], 137 mM NaCl and 0.1 % [v/v] Tween 20), containing 5 % fat-free dry milk for 0.45 µM membrane incubation and containing 3 % bovine serum albumin (BSA, AppliChem, Germany) for incubation with 0.2 µM membranes, which were washed three times with TBS-T afterwards. Incubation with primary antibodies was performed overnight at 4°C at 1/1000 dilution in TBS-T, containing 5 % BSA, except C-2, which was incubated in a dilution of 1/500 in TBS-T, containing 5 % fat-free dry milk. Finally, membranes were washed three times with TBS-T and incubated with either an anti-mouse-HRP secondary antibody for CREM C-2 or an anti-rabbit-HRP secondary antibody for the other primary antibodies (both from Cell Signalling Technology, USA) diluted 1/2000 in TBS-T, containing 5 % fat-free dry milk. After washing three times with TBS-T, immunodetection was performed with LumiGlo Reagent (Cell Signalling Technology, USA) using LAS-3000 (Fujifilm Lifescience, Germany). Band density was determined with ImageJ software (NIH, USA).

Measurement of zinc buffer capacity

$ZnSO_4$ (0 µM, 0.1 µM, 1 µM, 2 µM, 3 µM, 4 µM, 5 µM, 10 µM, 20 µM and 50 µM) and 1 µM Fluozin-3 tetrapotassium salt (ThermoFisher, Germany) were supplemented to HDAC1 buffer and 100 µL per well were distributed on a 96 well plate as triplicates. To determine minimal and maximal fluorescence as described before, 50 µM TPEN and 100 µM $ZnSO_4$ were pipetted to the HDAC1 buffer as triplicates, as well (Fig. S3). Subsequently, samples were incubated for 30 min at 37°C in the dark, followed by fluorescence measurement at the fluorescence plate reader Ultra 384 (Tecan, Germany). To determine the maximal fluorescence within the PP2A buffer, 3 µM $ZnSO_4$ were added. Due to the concentration optimum of FluoZin-3, the free zinc concentration for higher zinc concentrations was calculated with the respective formula afterwards. Free zinc concentrations in a higher range could not be reliably determined within the PP2A buffer. Fig. S3 A represents the free zinc in the reaction buffer with the experimental conditions wherein a 1/50 dilution of the PP2A preparation was used with a standard peptide as substrate whereas Fig. S3 B shows free zinc concentrations in the reaction buffer wherein a 1/20 dilution of the PP2A preparation was tested with a more physiological Rb peptide as substrate.

HDAC1 activity assay

The fluoregenic HDAC1 assay kit (BPS Bioscience, USA) was used according to the manufacturer's instructions. Enzyme activity was determined after supplementing 0 µM, 0.1 µM, 1 µM, 5 µM, 10 µM or 50 µM $ZnSO_4$ to the assay.

Preparation of active PP2A-B55α trimers

Ten 10 cm plates of HEK293T cells (ATCC) were each transfected with 5 µg of an N-terminally GFP-tagged human B55α expression vector, harboring a TEV protease cleavage site-encoding sequence in between the GFP and B55α coding sequences. 48 h after transfection, cells were lysed in NET lysis buffer (50 mM Tris-HCl [pH 7.4], 150 mM NaCl, 15 mM EDTA and 1 % Nonidet

P-40), complemented with protease inhibitor cocktail (Roche Applied Science, Germany) and centrifuged for 15 min at 13,000 g. The supernatants (lysates) were pooled and incubated with 25 µL of GFP-Trap® beads (ChromoTek, Germany) on a rotating wheel at 4°C for 1 h. Beads were washed four times with 1 mL NENT150 buffer (20 mM Tris-HCl [pH 7.4], 1 mM EDTA, 0.1 % Nonidet P-40, 25 % glycerol and 150 mM NaCl), and once in 1 mL assay buffer (50 mM Tris-HCl [pH 8.0] and 1 mM DTT). 20 µL of recombinant TEV-protease (2 µg/µL) was added to the beads in a volume of 80 µL assay buffer and incubated on a rotating wheel overnight at 4°C. After cleavage, the supernatant was removed and an equal volume of 100 % glycerol was added before long-term storage at -20°C. The presence of PP2A B55α, A and C subunits was verified by immunoblotting. The activity of each prep was pre-determined in a phosphatase assay, using a dilution series of the prep, different assay time points and different phospho-peptide substrates, allowing to precisely determine the linear range conditions.

PP2A activity assays

Activities were measured on two different phospho-peptides: R-K-T(p)-I-R-R (standard peptide) and I-N-G-S-P-R-T(p)-P-R-R-G-Q-N-R (Rb peptide); 2 mM stock solution of each (Synpeptide, China). The assay mixes were as follows: 10 µL of standard peptide, 25 µL of 50 mM Tris-HCl [pH 8.0] and 20 µL of diluted (1/50) PP2A-B55α phosphatase; or: 10 µL of Rb peptide, 25 µL of 50 mM Tris-HCl [pH 8.0] and 20 µL of diluted (1/20) PP2A-B55α phosphatase. After 10 min, resp. 20 min of incubation at 30°C, 25 µL were removed from these assay mixes and added to 50 µL Biomol®Green (Enzo Life Sciences, Germany) in a 96-well plate. After 30 min of incubation at RT, absorbance at 620 nm was measured in a microplate reader (Thermo Scientific MultiSkan, Germany). To test the effects of Zn^{2+} ions on PP2A-B55α activity, 5 µL of 50 mM Tris-HCl [pH 8.0] was replaced in the assay mixes by 5 µL of $ZnSO_4$ (resp. of 1/182, 1/910,

1/1820, 1/9100 and 1/91,000 dilutions of a stock solution of 100 mM $ZnSO_4$ in water). In all cases, the phospho-peptide was added to the assay mix as the last reagent, thereby allowing a short pre-incubation of PP2A-B55α and $ZnSO_4$ on ice before the reactions were effectively started at 30°C. The influence of TPEN with a final concentration of 50 µM on PP2A activity was comparably determined after 10 and 20 min.

Phosphatase activity assay in Jurkat cell lysates

To measure the alkaline phosphatase activity, $1x10^7$ cells/mL were resuspended in Hepes-reaction buffer (20 mM Hepes and 20 mM $MgCl_2$). Lysates were sonificated for 20 sec on ice using a Vibra Cell sonicator and were centrifuged for 3 min at 16,000 g. Supernatants were diluted 1:4 with reaction buffer and distributed with 100 µL/well on a 96 well plate. Subsequently, 1 µL *p*-nitrophenyl phosphate was added per well and incubated for 1 h at 37°C. Reaction was stopped with 100 µL NaOH and absorbance was measured using the Spark microplate reader (Tecan, Germany) at 405 nm and 492 nm as reference wavelength.

Statistical analysis

All experiments were performed in at least three independent replicates. Statistical significance of experimental results was calculated by Student's t-test using Excel and GraphPad software. Analyses of the porcine experiments were performed by using the unpaired t-test. Moderated t-statistics were calculated with the eBayes function from the limma package [37]. *P*-values of <0.05 were considered significant.

Results

Intracellular zinc levels are decreased after short-term and long-term zinc deficiency

To study the effect of zinc deficiency on reduced IL-2 production in T cells *in vitro*, one short-term and one long-term model was established. Thereby, zinc deficiency was induced either by the use of the zinc chelator TPEN for short-term zinc deficiency (three days) in HuT-78 and Jurkat T cells (Fig. 1 A, B) or by the use of Chelex-treated medium supplemented with 50 µg/L (0.174 nM) zinc sulfate ($ZnSO_4$), studying the effect of long-term zinc deficiency in Jurkat T cells after three weeks (Fig. 1 C-F). The TPEN concentration of 3 µM showed no toxic effects on HuT-78 (Fig. S1 A) and Jurkat T cells (Fig. S1 B), which was determined by cell viability measurements using propidium iodide (PI). Additionally, gated, structurally normal cells cultured in Chelex-treated medium showed no significantly more dead cells than cells in control medium, which was determined by PI measurements, as well (Fig. S1 C).

To confirm whether zinc levels were reduced in zinc-deficient samples, the intracellular zinc content was measured using the fluorescence probes FluoZin-3 AM (Fig. 1 A, B, E) and Zinpyr-1 (Fig. 1 F). The intracellular zinc level in HuT-78 T cells (Fig. 1 A) and in Jurkat T cells (Fig. 1 B, E, F) was significantly reduced in zinc deficiency in the short- and long-term model. Apart from fluorescence probes, flame atomic absorption spectrometry (AAS) analyses were used to determine the zinc content in the media used for cell cultivation in the long-term model, showing decreased zinc levels in the Chelex-treated medium compared to control medium (Fig. 1 C). Moreover, zinc concentrations were reduced within Jurkat T cells determined by AAS, as well (Fig. 1 D). Altogether, zinc levels were significantly reduced in samples after short-term as well as after long-term zinc deficiency compared to T cells cultivated in zinc adequate medium.

Thereby, the fluorescent probes only detect free zinc whereas AAS measurements give information about the total zinc content.

Zinc deficiency leads to decreased IL-2 expression

In a next step, the influence of zinc on IL-2 production in T cells was determined. After inducing short-term or long-term zinc deficiency, HuT-78 (Fig. 1 G) and Jurkat T cells (Fig. 1 H-K) were stimulated with phorbol-12-myristate-13-acetate (PMA) in combination with Calcimycin (Cal) for 24 h. To analyze the IL-2 production of long-term zinc-deficient Jurkat T cells, cells were moreover stimulated with phytohemagglutinin (PHA) (Fig. 1 I-K). Both stimulations revealed significantly reduced IL-2 levels in the supernatants of zinc-deficient T cells compared to control cells (Fig. 1 G-I). Apart from that, reduced IL-2 expression on RNA levels could be observed in unstimulated zinc-deficient cells (Fig. 1 J) and after 6 h and 24 h PMA/Cal stimulation in long-term zinc-deficient Jurkat T cells compared to control cells (Fig. 1 J, K).

To sum up, previously reported reduction of IL-2 expression by zinc-deficient T cells is confirmed in this study.

Long-term zinc deficiency alters zinc transporter expression

Zinc homeostasis needs to be tightly regulated and is ensured, for example, by zinc transporters. Since reduced intracellular zinc levels were observed within zinc-deficient T cells (Fig. 1), zinc transporter expression was analyzed on RNA level in the long-term zinc deficiency model (Fig. 2). All Zip importers were expressed by Jurkat T cells, except Zip12 (Fig. 2 A). Expression of the Zip transporters was increased in zinc-deficient T cells compared to control cells, showing significantly increased Zip10 expression (Fig. 2 A). In contrast, ZnT exporter expression was reduced, being significant for ZnT1, ZnT3 and ZnT8 after long-term zinc deficiency compared to control cells (Fig. 2 B). All ZnT transporters were expressed by Jurkat T cells except ZnT2 and

ZnT10. Zip as well as ZnT transporters are differentially expressed by T cells after long-term zinc deficiency compared to control cells, highlighting their important role in zinc homeostasis regulation.

CREMα expression of T cells is influenced by zinc

So far, it is not completely elucidated which molecular mechanisms cause the reduced IL-2 expression in zinc-deficient T cells. In T cells of SLE patients CREMα expression was increased, leading to inhibited IL-2 transcription [4]. Therefore, this transcription factor seems to be an interesting target molecule for the study of possible zinc effects. Indeed, CREMα expression is increased on RNA levels after short-term zinc deficiency in unstimulated and PMA/Cal-stimulated (6 h) HuT-78 (Fig. 3 A) and Jurkat T cells (Fig. 3 B). Furthermore, CREMα analysis in long-term zinc-deficient Jurkat T cells showed significantly increased CREMα expression after stimulation with PMA/Cal (6 h and 24 h) and PHA (24 h) on RNA levels (Fig. 3 C, D). However, not only on RNA, but also on protein levels, the amount of CREMα was increased in unstimulated long-term zinc-deficient T cells compared to control cells (Fig. 3 E, F).

Apart from *in vitro* studies, CREMα was analyzed in PBMC isolated from whole blood of zinc-supplemented pigs (*Sus scrofa domesticus) in vivo*, as well. The studied pigs received diets supplemented with either 0 ppm, 100 ppm or 2500 ppm zinc (Zn0, Zn100 or Zn2500) from zinc oxide (ZnO) for 1-2 weeks. Serum zinc was determined by inductively coupled plasma-mass spectrometry (ICP-MS), showing increased serum zinc levels in Zn2500 pigs compared to Zn0 and Zn100 pigs (Table S1). In addition, IL-2 production of porcine PBMC was analyzed in unstimulated and PMA/Cal-stimulated samples after 24 h (Table S2). Thereby, increased IL-2 production could be observed after supplementation with 2500 ppm zinc compared to Zn0 and

Zn100 pigs. Consistent with the previous findings, analysis of CREMα showed decreased CREMα levels after 2500 ppm zinc supplementation on protein levels (Fig. 3 G, H).

In summary, CREMα expression is increased in T cells on RNA levels after short-term (HuT-78 and Jurkat) and long-term (Jurkat) zinc deficiency, which is additionally confirmed on protein levels in the long-term model. Results obtained *in vitro* could be confirmed *in vivo*, as well. Here, we did not investigate the induction of an experimental zinc deficiency, but unsupplemented pigs, fed with the normal chow with a low zinc content, showed zinc serum levels of 52.42 ± 5.19 µg/dL (Table S1). Thus, they were zinc deficient in comparison to 2500 ppm supplemented pigs and to normal porcine serum values of 75.19 – 160.18 µg/dL [38].

Increased phosphatase activity after long-term zinc deficiency

As described in the previous section, zinc deficiency seems to be related to increased CREMα transcription factor expression. The transcription factor "specificity protein 1" (SP-1) is activated by protein phosphatase 2A (PP2A) and is able to bind the CREM promoter, thereby increasing CREM expression [10]. In the present study, phosphatase activity was measured in lysates of Jurkat T cells, which were cultivated for three weeks in either control or zinc-deficient medium. Complete phosphatase activity was slightly increased in zinc-deficient T cells compared to control T cells, however missing significance (Fig. 4 A). Therefore, the influence of zinc on the activity of purified PP2A enzyme was directly measured with the help of an enzyme assay. Thereby, a zinc-dependent inhibition of PP2A could be observed and the half maximal inhibitory concentration (IC_{50}) could be determined (Fig. 4 B, C). On the one hand, a standard peptide was used as substrate to determine the PP2A activity after zinc incubation, revealing an IC_{50} of 91.33 nM (Fig. 4 B). On the other hand, a more physiological peptide (Rb peptide) was used, showing a more zinc specific effect on PP2A activity with an IC_{50} of 20.53 nM (Fig. 4 C). The

IC_{50} was assessed by activity assay measurements normalized to free zinc in the reaction buffer using the standard peptide buffer (Fig. S3 A) and more physiological peptide buffer (Fig. S3 B). Additionally, the influence of zinc deficiency on PP2A activity was studied by the use of TPEN. Hereby, increased enzyme activity could be observed during time compared to control samples (Fig. 4 D). Thus, zinc deficiency promotes the activity of PP2A, likely resulting in increased SP-1 binding to the CREM promoter and thereby ensuring increased gene transcription.

Possible zinc targets in the upstream IL-2 and CREMα signaling pathways

Analysis of phosphorylated protein kinase A (PKA) substrate (Fig. 5 A, B), c-Fos (Fig. 5 C, D), S276 phosphorylation of the NF-κB subunit p65 (Fig. 5 E, F) and phosphorylation of T202/Y204 of the extracellular signal-regulated kinase (ERK) (Fig. 5 G, H) showed no significant differences in zinc-deficient compared to control cells. Moreover, analysis of H3S10 phosphorylation (Fig. 5 I, J) and H3K18 acetylation (Fig. 5 K, L) showed no significant differences in zinc-deficient compared to control cells. Therefore, CREMα transcription seems to be the primary response to zinc deficiency.

Metal-responsive transcription factor (MTF)-1 silencing does not alter IL-2 production.

MTF-1 senses zinc by stabilization of two of its six zinc fingers. Subsequently, MTF-1 is able to bind to the MRE site in target genes with the TGCRCNC sequence [30]. We analyzed the upstream region of the transcription start site (TSS) of the *IL2* gene (NG_016779) and identified an MRE sequence with TGCACTG at position 4085, approx. 1 kb upstream of the TSS. Interestingly, the CRE target sequence for CREMα with its 5'TGAC half-site shows similarities to the MRE sequence, being found within the IL-2 promoter at position -180 of the TSS [39]. To analyze a possible association between MTF-1 activity and IL-2 production, gene silencing was performed by use of small interfering (si)RNA. After transfection of Jurkat T cells with either negative control

siRNA or MTF-1 siRNA by electroporation, MTF-1 silencing was confirmed on RNA levels in the respective samples (Fig. 6 A). This was seen in decreased MTF-1 expression in MTF-1 siRNA-transfected unstimulated and stimulated cells compared to T cells transfected with negative control siRNA. However, analysis of the IL-2 production showed no differences in IL-2 levels in the supernatants of siRNA-transfected samples after stimulation (Fig. 6 B). Thereby, IL-2 regulation by MTF-1 via the MRE site within the IL-2 promoter can be excluded.

Zinc supplementation decreases HDAC1 activity while H3K9 acetylation is decreased in zinc-deficient T cells

Histone deacetylation of lysine residues by HDAC leads to repression of gene transcription [40]. Therefore, this enzyme class represents another interesting target to analyze the effect of zinc in the context of altered IL-2 production. In the current study, increased HDAC1 expression on RNA levels was observed in zinc-deficient Jurkat T cells compared to zinc adequate control cells (Fig. 7 A). Zinc not only affected the expression on RNA levels, but also the enzyme activity of HDAC1 (Fig. 7 B, C). In detail, zinc supplementation significantly decreased HDAC1 activity, resulting in almost complete inhibition of the enzyme after addition of 50 µM $ZnSO_4$ (Fig. 7 B), which resembles a concentration of 102.02 nM free zinc within the buffer. Furthermore, the IC_{50} of zinc on HDAC1 activity was determined, revealing an IC_{50} of 0.26 nM free zinc (Fig. 7 C). Again, the IC_{50} was assessed by activity assay measurements normalized to free zinc in the HDAC1 reaction buffer (Fig. S4). Additionally, H3K9 was significantly deacetylated in Jurkat T cells after long-term zinc deficiency compared to control cells (Fig. 7 D, E).

Apart from acetylation, the methylation pattern of Jurkat T cell DNA was analyzed, possibly representing another zinc-affected epigenetic regulatory mechanism, which might lead to impaired IL-2 expression. However, methylation analysis of the Jurkat T cell genome did not show any

significant differences between DNA of zinc-deficient and control T cells in the *IL2* gene (adjusted *p*-value = 0.86, Table S3).

In summary, HDAC1 expression was increased on RNA levels in zinc-deficient compared to control T cells. Zinc supplementation caused inhibition of HDAC1 enzyme activity and an IC_{50} could be determined with a physiological value of 0.26 nM zinc. Accordingly, increased H3K9 deacetylation leading to increased CREMα binding could be observed in zinc-deficient T cells.

Discussion

Zinc deficiency negatively affects IL-2 expression in T cells, leading to impaired immune functions [41,42]. However, the responsible underlying mechanisms are not elucidated so far. Therefore, it was our aim to investigate molecular targets, linking zinc deficiency to reduced IL-2 expression.

Initially, zinc deficiency after incubation with TPEN- or Chelex-treated medium was confirmed in HuT-78 and Jurkat T cells. We directly detected either intracellular free zinc by a fluorescence marker or determined the total zinc concentration by AAS. Additionally, the expression of metallothionine was probably also reduced under zinc deficiency, as this has already been shown in Jurkat T cells after TPEN treatment [43]. For clinical use, the direct detection of zinc is also the recommended method [44]. Apart from reduced intracellular zinc levels, altered zinc transporter expression was observed in zinc-deficient compared to control T cells, assuming adaptation of the cell to the zinc-starving conditions. The exporter ZnT1 is ubiquitously expressed within plasma membranes, especially in leukocytes but also in erythrocytes and other cell types [45], ensuring zinc export into the extracellular space [34]. ZnT3 transporter expression was found in leukocytes as well and also in the brain, testis and pancreas. Its cellular localization is particularly described to synaptic vesicles of neurons [34,45]. Thus, ZnT3 might be localized to vesicles in T cells, too. To

date, zincosomes are described in $CD4^+$ T cells which might harbor ZnT3 and ZnT8 transporters [46]. The third altered ZnT exporter ZnT8 is found within membranes of secretory vesicles in leukocytes and other tissues. This transporter is involved in the formation of zinc/insulin crystals, in the maturation and storage of insulin and represents the major autoantigen in the development of type I diabetes [34,45]. In contrast, expression of the Zip10 importer was significantly increased. Zip10 is localized to the plasma membrane of leukocytes and was so far especially found in human B and murine T cells [18,47]. Other zinc transporters are also important for T cell activation [48] but were not significantly affected by zinc deficiency and are therefore not further discussed.

We identified one MRE binding site in the upstream sequence of the IL-2 TSS, which is localized in proximity to the CRE site. The MRE sequence is usually targeted by MTF-1 and MTF-1 silencing resulting in its reduced transcription, as confirmed on RNA levels. However, IL-2 production was not affected, excluding an association of altered IL-2 transcription by differential MTF-1 binding to the IL-2 promoter.

Aside from the CRE and MRE sites, the IL-2 promoter harbors several transcription factor binding sites, being important for *IL2* gene transcription, as for example one NF-κB binding site. In zinc-deficient HuT-78 T cells, NF-κB activation is decreased which might lead to subsequent decreased IL-2 expression. On the molecular level, zinc affects phosphorylation of the inhibitor of kappa B and IκB kinase, NF-κB translocation to the nucleus and NF-κB DNA binding [49]. In contrast, zinc supplementation of zinc-deficient murine T cells increased phosphorylation of the mitogen-associated protein kinase p38 and the NF-κB subunit p65, going along with increased IL-2 production [18]. However, only slight decreases in p65 phosphorylation were observed in the present study, missing significance and therefore not completely explaining zinc-affected IL-2 expression. Furthermore, changes of IL-2 mRNA levels seem rather to be the result of altered cytokine gene expression than to be the result of zinc-affected RNA stability. This was confirmed by analyses

performed on the transcriptional level by using the mRNA synthesis inhibitor actinomycin D [50]. This hypothesis can be supported by our finding of zinc-affected CREMα levels, indicating gene expression regulation on epigenetic levels (Fig. 8). High CREMα levels ensure increased binding to the -180 CRE site within the IL-2 promoter, thereby reducing IL-2 transcription [8,9]. In the present study, CREMα levels were not only increased in zinc-deficient T cells *in vitro*. *In vivo*, the amount of CREMα was reduced, being paralleled by increased IL-2 production in pigs fed a diet supplemented with 2500 ppm zinc compared to pigs fed either a diet left unsupplemented or supplemented with 100 ppm zinc. Comparison of the porcine, human and murine genomes indicates a closer relationship between the porcine and human genomes than between the murine and human genomes. These similarities comprise especially immunologically associated genes, showing 80 % similarities between humans and pigs, as seen in the frequency of orthology preservation [51]. Thus, the use of a pig model seems to represent an improved model in the study of human immunological questions, allowing adaptation of obtained results to the human system. The serum zinc level measured in Zn2500 pigs resembles the physiological serum zinc levels observed in humans (83-102 µg/dL zinc) [52–54]. SLE patients have reduced serum zinc concentrations compared to healthy controls [5–7], indicating an interesting association of zinc with altered CREMα and IL-2 levels.

Protein phosphatases are inhibited by zinc and therefore increased activity can be expected in zinc-deficient samples [42]. Thus, stronger PP2A activity might cause higher S59 dephosphorylation of SP-1, resulting in increased SP-1 binding to the CREM promoter. This in turn, enhances CREM transcription, which was previously described in SLE T cells [10,55]. Direct inhibitory effects of zinc (100 µM) on purified full-length PP2A enzyme activity was already shown by [56]. However, this group did not determine an IC_{50} value and did not normalize their result to the intracellular free zinc levels. In the present study we were able to detect zinc-dependent inhibition of PP2A,

revealing an IC_{50} of 20.53 nM free zinc by using the more physiological Rb peptide as substrate compared to an IC_{50} of 91.33 nM by the use of a standard peptide. Measurement of the zinc buffer capacity was hindered due to the presence of dithiothreitol (DTT) in the reaction buffer, influencing the intracellular zinc content. Additionally, DTT might interfere with the probe. This might explain the higher zinc concentration obtained for the IC_{50} value compared to the intracellular zinc amount measured within the cells. Moreover, depending on the zinc accumulation and PP2A localization within the cell, zinc concentrations might actually be higher as measured by FluoZin-3 AM and Zinpyr-1.

In addition to this observed zinc-dependent inhibition, we were able to detect increased PP2A activity upon zinc deficiency. Nevertheless, this could not be observed in Jurkat cell lysates, likely due to saturation of the enzyme with zinc within the cell. This saturation might prevent any measurable effect, apart from the unspecificity of this assay due to the measurement of the phosphatase activity in general, instead of specific PP2A measurement. These results indicate that PP2A activity is higher under zinc-deficient conditions and interestingly, increased CREMα levels were already observed in unstimulated cells. By this, CREMα might bind to the IL-2 promoter in zinc-deficient unstimulated cells and cell stimulation results in lower maximal IL-2 levels compared to zinc adequate control cells. Binding of CREMα to immune response gene promoters, such as the IL-2 promoter, led to active HDAC1 recruitment, enhanced deacetylation of histones and subsequent transcriptional repression [57].

CREMα transported HDAC1 to the -180 CRE site within the IL-2 promoter, causing increased H3K18 deacetylation followed by inhibited IL-2 transcription [58]. HDAC1 belongs to the class I enzymes, being zinc-dependent and is moreover essential for efficient generation of thymocytes and peripheral T cells in mice [59,60]. This study demonstrates the zinc-induced inhibition of HDAC1 activity, conversely resulting in increased activity under zinc deficiency. 50 % HDAC1 inhibition

(IC_{50}) was obtained in the presence of 0.26 nM free Zn^{2+}. The intracellular zinc content measured with FluoZin-3 AM in zinc adequate control Jurkat T cells showed 0.22 nM ± 0.02 nM Zn^{2+}, indicating inhibitory properties on HDAC1. In contrast, the intracellular free zinc concentration within zinc-deficient T cells comprised only 0.10 nM ± 0.05 nM Zn^{2+}, resulting in higher HDAC1 activity. This in turn might cause the observed increases in H3K9 deacetylation, leading to a more condensed chromatin structure, thus reducing IL-2 transcription.

Recently, HDAC1 was related to experimental autoimmune encephalomyelitis (EAE), which represents an animal model for the study of multiple sclerosis. T cell specific HDAC1 deletion protected EAE development, representing an interesting target enzyme in the treatment of MS. However, $CD4^+$ T cells lacking HDAC1 were still able to differentiate into T helper (Th)17 cells [61]. Furthermore, zinc supplementation positively affected disease development of EAE by decreasing Th17 cells and increasing inducible regulatory T cells [62]. With these two different studies our observation of zinc-inhibited HDAC1 activity highlights once again the importance of an adequate zinc status in relation to autoimmune diseases. Histone deacetylase inhibitors possess beneficial effects on various diseases, as seen in an allergic rhinitis mouse model. By use of an HDAC1 inhibitor, H3K9 acetylation was increased in the nasal mucosa paralleled by increased IL-2 levels in the murine serum [63]. Apart from that, zinc supplementation of broiler chickens was associated with increased H3K9 acetylation in their progeny [64]. Those studies support the influence of zinc on HDAC1 enzyme activity.

Besides acetylation, chromatin remodeling of the IL-2 promoter region paralleled by differentiated methylation was related to IL-2 transcription regulation in former studies [65–67]. However, analysis of the methylation pattern of the *IL2* gene performed in the present study showed no significant alterations between control and zinc-deficient T cells, thus excluding differential methylation as a cause of reduced IL-2 transcription under zinc-deficient conditions.

Especially the elderly appears to be more prone to infections, likely due to malnutrition. Immune responses are assumed to decline with age which in turn increases the incidence of cancer, infections, autoimmune diseases and others [68]. Almost 60 % of the elderly in the United States of America are estimated to be zinc-deficient [69]. Furthermore, cytokine production and T cell subsets were found to be influenced by zinc in this population [70]. In mildly zinc-deficient elderly, decreased IL-2 activity of Th cells was observed and also a higher incidence of T cell anergy [71]. Additionally, Th1 cells of human subjects, who were brought experimentally to mild zinc deficiency, produced less IL-2 as well, going along with impaired Th1 functions [11]. Several studies describe increased HDAC1 activity in the livers of old mice and decreased H3K9 acetylation in the livers of old rats [72,73]. One possible explanation of reduced IL-2 expression in zinc-deficient elderly might therefore be increased CREMα levels, which recruits more active HDAC1 enzyme to the IL-2 promoter region, consequently leading to decreased IL-2 transcription. IL-2 is especially important for the maintenance of Tregs and the elimination of self-reactive T cells mediated by activation-induced cell death. Thus, a decrease in bioavailable IL-2 decreases the activation of T cells and natural killer cells and can disturb peripheral tolerance and immune regulation. Even the very comparable IL-15 does not cover these functions [74].

Zinc supplementation of elderly might therefore be beneficial. Beneficial effects of zinc supplementation of elderly were already shown, which were related to decreased spontaneous cytokine release with great impact on reduced IL-6 levels and restored production of Th1 cytokines [75].

In conclusion, we were able to identify a molecular link between zinc and impaired IL-2 production in T cells using one zinc-deficient short-term and one long-term model *in vitro* and, additionally, using zinc-deficient pigs supplemented with zinc *in vivo*. This link is represented by the transcription factor CREMα, being increased after zinc deficiency, due to enhanced PP2A

activity (IC_{50}=20.53 nM), and decreased after zinc supplementation, leading to altered IL-2 expression (Fig. 8). Thereby, regulation of IL-2 expression on epigenetic levels is highlighted. Under zinc-deficient conditions, Zip10 importer expression is increased, in contrast to decreased ZnT1, ZnT3 and ZnT8 exporter expression. Moreover, HDAC1 activity is higher in zinc-deficient T cells, as seen by increased H3K9 deacetylation, making the DNA inaccessible for transcription. Inhibitory effects of zinc on HDAC1 activity were observed as well, revealing an IC_{50} in the presence of 0.26 nM free Zn^{2+}.

However, a limitation of this study is, that the effect of zinc on SP-1 phosphorylation can only be assumed due to the altered PP2A activity. The use of an adequate antibody [10] is one possibility to directly investigate the impact on SP-1 phosphorylation in future studies, however, this antibody is no longer available from this group. Furthermore, the results may not completely represent the effects in humans, as we have studied the mechanism in human T cell lines and PBMC and *in vivo* in pigs. Additionally, Zip1 and ZnT1 expression upon zinc treatment vary a lot across studies [76]. Therefore, results on zinc transporter expression obtained in the two T cell lines might not be consistent in other cell types or primary cells.

To our knowledge, expression of CREMα is so far especially analyzed in SLE suffering patients. On basis of the herein obtained results, it might be interesting to extend the analysis of CREMα expression to populations which are prone to zinc deficiency, such as the elderly or vegetarians. With knowledge of this zinc-affected molecular link it might be possible to beneficially influence impaired IL-2 expression to ensure proper immunological functions.

Acknowledgments

We would like to thank Prof. Hanne Damgaard Poulsen and Tina Sørensen Dalgaard (Ph.D.) from Aarhus University (Denmark) for the good cooperation with the pig experiments. Funding: L.R.

is member of Zinc-Net. This work was supported by Zinc-Net [Cost Action TD1304], the Danish Council for Independent Research, Technology and Production Sciences [grant number: DFF-1337-00135], Aarhus University and the KU Leuven Research Fund [C24/17/073].

Statement of Authorship

V.K. and L.R. designed research. V.K. performed most of the experiments. I.W. performed AAS measurements. K.B. provided ICP-MS data and pigs. V.J. produced PP2A enzyme and performed PP2A activity measurements. V.K., J.H., W.W. and L.R. analyzed data. V.K., J.W. and L.R. wrote the manuscript. All authors reviewed the manuscript.

Conflict of Interest

The authors declare no conflict of interest.

References

1. Kim HP, Imbert J, Leonard WJ. Both integrated and differential regulation of components of the IL-2/IL-2 receptor system. *Cytokine Growth Factor Rev* 2006; **17:** 349–366; DOI: 10.1016/j.cytogfr.2006.07.003.

2. Bayer AL, Pugliese A, Malek TR. The IL-2/IL-2R system: from basic science to therapeutic applications to enhance immune regulation. *Immunol Res* 2013; **57:** 197–209; DOI: 10.1007/s12026-013-8452-5.

3. Delmas V, Laoide BM, Masquilier D, Groot RP de, Foulkes NS, Sassone-Corsi P. Alternative usage of initiation codons in mRNA encoding the cAMP-responsive-element modulator generates regulators with opposite functions. *Proc Natl Acad Sci U S A* 1992; **89:** 4226–4230; DOI: 10.1073/pnas.89.10.4226.

4. Tenbrock K, Tsokos GC. Transcriptional regulation of interleukin 2 in SLE T cells. *Int Rev Immunol* 2004; **23:** 333–345; DOI: 10.1080/08830180490452558.

5. Sahebari M, Abrishami-Moghaddam M, Moezzi A *et al.* Association between serum trace element concentrations and the disease activity of systemic lupus erythematosus. *Lupus* 2014; **23:** 793–801; DOI: 10.1177/0961203314530792.

6. Tóth CN, Baranyai E, Csípő I *et al.* Elemental Analysis of Whole and Protein Separated Blood Serum of Patients with Systemic Lupus Erythematosus and Sjögren's Syndrome. *Biol Trace Elem Res* 2017; **179:** 14–22; DOI: 10.1007/s12011-017-0945-y.

7. Yilmaz A, Sari RA, Gundogdu M, Kose N, Dag E. Trace elements and some extracellular antioxidant proteins levels in serum of patients with systemic lupus erythematosus. *Clin Rheumatol* 2005; **24:** 331–335; DOI: 10.1007/s10067-004-1028-y.

8. Kyttaris VC, Wang Y, Juang YT, Weinstein A, Tsokos GC. CAMP response element modulator a expression in patients with systemic lupus erythematosus. *Lupus* 2006; **15:** 840–844; DOI: 10.1177/0961203306069985.

9. Solomou EE, Juang YT, Gourley MF, Kammer GM, Tsokos GC. Molecular basis of deficient IL-2 production in T cells from patients with systemic lupus erythematosus. *J Immunol* 2001; **166:** 4216–4222; DOI: 10.4049/jimmunol.166.6.4216.

10. Juang Y-T, Rauen T, Wang Y *et al.* Transcriptional activation of the cAMP-responsive modulator promoter in human T cells is regulated by protein phosphatase 2A-mediated dephosphorylation of SP-1 and reflects disease activity in patients with systemic lupus erythematosus. *J Biol Chem* 2011; **286:** 1795–1801; DOI: 10.1074/jbc.M110.166785.

11. Beck FW, Prasad AS, Kaplan J, Fitzgerald JT, Brewer GJ. Changes in cytokine production and T cell subpopulations in experimentally induced zinc-deficient humans. *Am J Physiol* 1997; **272:** E1002-7; DOI: 10.1152/ajpendo.1997.272.6.E1002.

12. Haase H, Rink L. Functional significance of zinc-related signaling pathways in immune cells. *Annu Rev Nutr* 2009; **29:** 133–152; DOI: 10.1146/annurev-nutr-080508-141119.

13. Prasad AS, Meftah S, Abdallah J *et al.* Serum thymulin in human zinc deficiency. *J Clin Invest* 1988; **82:** 1202–1210; DOI: 10.1172/JCI113717.

14. Rink L, Gabriel P. Zinc and the immune system. *Proc Nutr Soc* 2000; **59:** 541–552; DOI: 10.1017/s0029665100000781.

15. Vallee BL, Falchuk KH. The biochemical basis of zinc physiology. *Physiol Rev* 1993; **73:** 79–118; DOI: 10.1152/physrev.1993.73.1.79.

16. Kloubert V, Rink L. Zinc as a micronutrient and its preventive role of oxidative damage in cells. *Food Funct* 2015; **6:** 3195–3204; DOI: 10.1039/c5fo00630a.

17. Radtke F, Heuchel R, Georgiev O *et al.* Cloned transcription factor MTF-1 activates the mouse metallothionein I promoter. *EMBO J* 1993; **12:** 1355–1362.

18. Daaboul D, Rosenkranz E, Uciechowski P, Rink L. Repletion of zinc in zinc-deficient cells strongly up-regulates IL-1β-induced IL-2 production in T-cells. *Metallomics* 2012; **4:** 1088–1097; DOI: 10.1039/c2mt20118f.

19. Prasad AS, Beck FWJ, Bao B *et al.* Zinc supplementation decreases incidence of infections in the elderly: effect of zinc on generation of cytokines and oxidative stress. *Am J Clin Nutr* 2007; **85:** 837–844; DOI: 10.1093/ajcn/85.3.837.

20. Prasad AS, Beck FW, Kaplan J *et al.* Effect of zinc supplementation on incidence of infections and hospital admissions in sickle cell disease (SCD). *Am J Hematol* 1999; **61:** 194–202; DOI: 10.1002/(sici)1096-8652(199907)61:3<194::aid-ajh6>3.0.co;2-c.

21. Tybirk, P., Sloth, N. & Jørgensen, L. *Danish Nutrient Standards* (Copenhagen, 2014), http://www.pigresearchcentre.dk/Research/Nutrient%20standards.aspx.

22. Kloubert V, Blaabjerg K, Dalgaard TS, Poulsen HD, Rink L, Wessels I. Influence of zinc supplementation on immune parameters in weaned pigs. *J Trace Elem Med Biol* 2018; **49:** 231–240; DOI: 10.1016/j.jtemb.2018.01.006.

23. Mayer LS, Uciechowski P, Meyer S, Schwerdtle T, Rink L, Haase H. Differential impact of zinc deficiency on phagocytosis, oxidative burst, and production of pro-inflammatory cytokines by human monocytes. *Metallomics* 2014; **6:** 1288–1295; DOI: 10.1039/c4mt00051j.

24. Yui S, Nakatani Y, Hunter MJ, Chazin WJ, Yamazaki M. Implication of extracellular zinc exclusion by recombinant human calprotectin (MRP8 and MRP14) from target cells in its apoptosis-inducing activity. *Mediators Inflamm* 2002; **11:** 165–172; DOI: 10.1080/09622935020138208.

25. Haase H, Ober-Blöbaum JL, Engelhardt G *et al.* Zinc signals are essential for lipopolysaccharide-induced signal transduction in monocytes. *J Immunol* 2008; **181:** 6491–6502; DOI: 10.4049/jimmunol.181.9.6491.

26. Haase H, Hebel S, Engelhardt G, Rink L. Flow cytometric measurement of labile zinc in peripheral blood mononuclear cells. *Anal Biochem* 2006; **352:** 222–230; DOI: 10.1016/j.ab.2006.02.009.

27. Krezel A, Maret W. Zinc-buffering capacity of a eukaryotic cell at physiological pZn. *J Biol Inorg Chem* 2006; **11:** 1049–1062; DOI: 10.1007/s00775-006-0150-5.

28. Burdette SC, Walkup GK, Spingler B, Tsien RY, Lippard SJ. Fluorescent sensors for Zn(2+) based on a fluorescein platform: synthesis, properties and intracellular distribution. *J Am Chem Soc* 2001; **123:** 7831–7841; DOI: 10.1021/ja010059l.

29. Hönscheid A, Dubben S, Rink L, Haase H. Zinc differentially regulates mitogen-activated protein kinases in human T cells. *J Nutr Biochem* 2012; **23:** 18–26; DOI: 10.1016/j.jnutbio.2010.10.007.

30. Hardyman JEJ, Tyson J, Jackson KA *et al.* Zinc sensing by metal-responsive transcription factor 1 (MTF1) controls metallothionein and ZnT1 expression to buffer the sensitivity of the transcriptome response to zinc. *Metallomics* 2016; **8:** 337–343; DOI: 10.1039/c5mt00305a.

31. Faneyte IF, Kristel PM, van de Vijver MJ. Determining MDR1/P-glycoprotein expression in breast cancer. *Int J Cancer* 2001; **93:** 114–122; DOI: 10.1002/1097-0215(20010701)93:1<114::aid-ijc1309>3.0.co;2-j.

32. Dubben S, Hönscheid A, Winkler K, Rink L, Haase H. Cellular zinc homeostasis is a regulator in monocyte differentiation of HL-60 cells by 1 alpha,25-dihydroxyvitamin D3. *J Leukoc Biol* 2010; **87:** 833–844; DOI: 10.1189/jlb.0409241.

33. Leung KW, Liu M, Xu X, Seiler MJ, Barnstable CJ, Tombran-Tink J. Expression of ZnT and ZIP zinc transporters in the human RPE and their regulation by neurotrophic factors. *Invest Ophthalmol Vis Sci* 2008; **49:** 1221–1231; DOI: 10.1167/iovs.07-0781.

34. Overbeck S, Uciechowski P, Ackland ML, Ford D, Rink L. Intracellular zinc homeostasis in leukocyte subsets is regulated by different expression of zinc exporters ZnT-1 to ZnT-9. *J Leukoc Biol* 2008; **83:** 368–380; DOI: 10.1189/jlb.0307148.

35. Krusche CA, Vloet AJ, Classen-Linke I, Rango U von, Beier HM, Alfer J. Class I histone deacetylase expression in the human cyclic endometrium and endometrial adenocarcinomas. *Hum Reprod* 2007; **22:** 2956–2966; DOI: 10.1093/humrep/dem241.

36. Livak KJ, Schmittgen TD. Analysis of relative gene expression data using real-time quantitative PCR and the 2(-Delta Delta C(T)) Method. *Methods* 2001; **25:** 402–408; DOI: 10.1006/meth.2001.1262.

37. Ritchie ME, Phipson B, Di Wu *et al.* limma powers differential expression analyses for RNA-sequencing and microarray studies. *Nucleic Acids Res* 2015; **43:** e47; DOI: 10.1093/nar/gkv007.

38. Elbers AR, Geudeke MJ, van Rossem H, Kroon MC, Counotte GH. Haematology and biochemistry reference values for sows kept under modern management conditions. *Vet Q* 1994; **16:** 127–130; DOI: 10.1080/01652176.1994.9694433.

39. Rauen T, Hedrich CM, Tenbrock K, Tsokos GC. cAMP responsive element modulator: a critical regulator of cytokine production. *Trends Mol Med* 2013; **19:** 262–269; DOI: 10.1016/j.molmed.2013.02.001.

40. Haberland M, Montgomery RL, Olson EN. The many roles of histone deacetylases in development and physiology: implications for disease and therapy. *Nat Rev Genet* 2009; **10:** 32–42; DOI: 10.1038/nrg2485.

41. Gammoh NZ, Rink L. Zinc in Infection and Inflammation. *Nutrients* 2017; **9**; DOI: 10.3390/nu9060624.

42. Haase H, Rink L. Zinc signals and immune function. *Biofactors* 2014; **40:** 27–40; DOI: 10.1002/biof.1114.

43. Haase H, Mazzatti DJ, White A *et al.* Differential gene expression after zinc supplementation and deprivation in human leukocyte subsets. *Molecular medicine (Cambridge, Mass.)* 2007; **13:** 362–370; DOI: 10.2119/2007–00049.Haase.

44. Lowe NM, Fekete K, Decsi T. Methods of assessment of zinc status in humans: a systematic review. *Am J Clin Nutr* 2009; **89:** 2040S-2051S; DOI: 10.3945/ajcn.2009.27230G.

45. Huang L, Tepaamorndech S. The SLC30 family of zinc transporters - a review of current understanding of their biological and pathophysiological roles. *Mol Aspects Med* 2013; **34:** 548–560; DOI: 10.1016/j.mam.2012.05.008.

46. Yu M, Lee W-W, Tomar D *et al.* Regulation of T cell receptor signaling by activation-induced zinc influx. *J Exp Med* 2011; **208:** 775–785; DOI: 10.1084/jem.20100031.

47. Hojyo S, Miyai T, Fujishiro H *et al.* Zinc transporter SLC39A10/ZIP10 controls humoral immunity by modulating B-cell receptor signal strength. *Proc Natl Acad Sci U S A* 2014; **111:** 11786–11791; DOI: 10.1073/pnas.1323557111.

48. Maywald M, Wessels I, Rink L. Zinc Signals and Immunity. *International journal of molecular sciences* 2017; **18**; DOI: 10.3390/ijms18102222.

49. Prasad AS, Bao B, Beck FW, Sarkar FH. Zinc activates NF-kappaB in HUT-78 cells. *J Lab Clin Med* 2001; **138:** 250–256; DOI: 10.1067/mlc.2001.118108.

50. Bao B, Prasad AS, Beck FWJ, Godmere M. Zinc modulates mRNA levels of cytokines. *Am J Physiol Endocrinol Metab* 2003; **285:** E1095-102; DOI: 10.1152/ajpendo.00545.2002.

51. Dawson HD. A Comparative Assessment of the Pig, Mouse and Human Genomes. In: McAnulty PA, Dayan AD, Ganderup NC, Hastings KL (eds). *The Minipig in Biomedical Research.* CRC Press: Boca Raton, FL, USA, 2011, pp. 323-342.

52. Chen WJ, Zhao CY, Zheng TL. Comparison of zinc contents in human serum and plasma. *Clin Chim Acta* 1986; **155:** 185–187; DOI: 10.1016/0009-8981(86)90282-2.

53. Folin M, Contiero E, Vaselli GM. Zinc content of normal human serum and its correlation with some hematic parameters. *Biometals* 1994; **7:** 75–79; DOI: 10.1007/bf00205198.

54. Kosman DJ, Henkin RI. Plasma and serum zinc concentrations. *Lancet* 1979; **1:** 1410; DOI: 10.1016/s0140-6736(79)92047-6.

55. Vicart A, Lefebvre T, Imbert J, Fernandez A, Kahn-Perlès B. Increased chromatin association of Sp1 in interphase cells by PP2A-mediated dephosphorylations. *J Mol Biol* 2006; **364:** 897–908; DOI: 10.1016/j.jmb.2006.09.036.

56. Xiong Y, Luo D-J, Wang X-L *et al.* Zinc binds to and directly inhibits protein phosphatase 2A in vitro. *Neurosci Bull* 2015; **31:** 331–337; DOI: 10.1007/s12264-014-1519-z.

57. Tenbrock K, Juang Y-T, Leukert N, Roth J, Tsokos GC. The transcriptional repressor cAMP response element modulator alpha interacts with histone deacetylase 1 to repress promoter activity. *J Immunol* 2006; **177:** 6159–6164; DOI: 10.4049/jimmunol.177.9.6159.

58. Hedrich CM, Rauen T, Tsokos GC. cAMP-responsive element modulator (CREM)α protein signaling mediates epigenetic remodeling of the human interleukin-2 gene: implications in systemic lupus erythematosus. *J Biol Chem* 2011; **286:** 43429–43436; DOI: 10.1074/jbc.M111.299339.

59. Choudhary C, Weinert BT, Nishida Y, Verdin E, Mann M. The growing landscape of lysine acetylation links metabolism and cell signalling. *Nat Rev Mol Cell Biol* 2014; **15:** 536–550; DOI: 10.1038/nrm3841.

60. Tschismarov R, Firner S, Gil-Cruz C *et al.* HDAC1 controls CD8+ T cell homeostasis and antiviral response. *PLoS ONE* 2014; **9:** e110576; DOI: 10.1371/journal.pone.0110576.

61. Göschl L, Preglej T, Hamminger P *et al.* A T cell-specific deletion of HDAC1 protects against experimental autoimmune encephalomyelitis. *J Autoimmun* 2018; **86:** 51–61; DOI: 10.1016/j.jaut.2017.09.008.

62. Rosenkranz E, Maywald M, Hilgers R-D *et al.* Induction of regulatory T cells in Th1-/Th17-driven experimental autoimmune encephalomyelitis by zinc administration. *J Nutr Biochem* 2016; **29:** 116–123; DOI: 10.1016/j.jnutbio.2015.11.010.

63. Wang J, Wen L, Wang Y, Chen F. Therapeutic Effect of Histone Deacetylase Inhibitor, Sodium Butyrate, on Allergic Rhinitis In Vivo. *DNA Cell Biol* 2016; **35:** 203–208; DOI: 10.1089/dna.2015.3037.

64. Li C, Guo S, Gao J *et al.* Maternal high-zinc diet attenuates intestinal inflammation by reducing DNA methylation and elevating H3K9 acetylation in the A20 promoter of offspring chicks. *J Nutr Biochem* 2015; **26:** 173–183; DOI: 10.1016/j.jnutbio.2014.10.005.

65. Murayama A, Sakura K, Nakama M *et al.* A specific CpG site demethylation in the human interleukin 2 gene promoter is an epigenetic memory. *EMBO J* 2006; **25:** 1081–1092; DOI: 10.1038/sj.emboj.7601012.

66. Rao S, Procko E, Shannon MF. Chromatin remodeling, measured by a novel real-time polymerase chain reaction assay, across the proximal promoter region of the IL-2 gene. *J Immunol* 2001; **167:** 4494–4503; DOI: 10.4049/jimmunol.167.8.4494.

67. Ward SB, Hernandez-Hoyos G, Chen F, Waterman M, Reeves R, Rothenberg EV. Chromatin remodeling of the interleukin-2 gene: distinct alterations in the proximal versus distal enhancer regions. *Nucleic Acids Res* 1998; **26:** 2923–2934; DOI: 10.1093/nar/26.12.2923.

68. Chandra RK. Nutritional regulation of immunity and risk of infection in old age. *Immunology* 1989; **67:** 141–147.

69. Briefel RR, Bialostosky K, Kennedy-Stephenson J, McDowell MA, Ervin RB, Wright JD. Zinc intake of the U.S. population: findings from the third National Health and Nutrition Examination Survey, 1988-1994. *J Nutr* 2000; **130:** 1367S-73S; DOI: 10.1093/jn/130.5.1367S.

70. Cakman I, Rohwer J, Schütz RM, Kirchner H, Rink L. Dysregulation between TH1 and TH2 T cell subpopulations in the elderly. *Mech Ageing Dev* 1996; **87:** 197–209; DOI: 10.1016/0047-6374(96)01708-3.

71. Prasad AS. Zinc in growth and development and spectrum of human zinc deficiency. *J Am Coll Nutr* 1988; **7:** 377–384; DOI: 10.1080/07315724.1988.10720255.

72. Kawakami K, Nakamura A, Ishigami A, Goto S, Takahashi R. Age-related difference of site-specific histone modifications in rat liver. *Biogerontology* 2009; **10:** 415–421; DOI: 10.1007/s10522-008-9176-0.

73. Wang G-L, Salisbury E, Shi X, Timchenko L, Medrano EE, Timchenko NA. HDAC1 cooperates with C/EBPalpha in the inhibition of liver proliferation in old mice. *J Biol Chem* 2008; **283:** 26169–26178; DOI: 10.1074/jbc.M803544200.

74. Waldmann TA. The shared and contrasting roles of IL2 and IL15 in the life and death of normal and neoplastic lymphocytes: implications for cancer therapy. *Cancer immunology research* 2015; **3:** 219–227; DOI: 10.1158/2326-6066.CIR-15-0009.

75. Kahmann L, Uciechowski P, Warmuth S *et al.* Zinc supplementation in the elderly reduces spontaneous inflammatory cytokine release and restores T cell functions. *Rejuvenation Res* 2008; **11:** 227–237; DOI: 10.1089/rej.2007.0613.

76. Hennigar SR, Kelley AM, McClung JP. Metallothionein and Zinc Transporter Expression in Circulating Human Blood Cells as Biomarkers of Zinc Status: a Systematic Review. *Adv Nutr* 2016; **7:** 735–746; DOI: 10.3945/an.116.012518.

Figure Captions

Fig. 1. Zinc levels and IL-2 expression are decreased in zinc-deficient (ZnD) conditions.

(A and B) Intracellular zinc levels in HuT-78 (A) and Jurkat (B) T cells after three days in control or zinc-deficient conditions (short-term model) determined by flow cytometry using FluoZin-3 AM (n = 4 for each cell line).

(C and D) Zinc concentrations in the used control and Chelex-treated media (C, n = 14) and in Jurkat T cells after three weeks in zinc deficiency (D, n = 4) measured by flame atomic absorption spectrometry (AAS).

(E and F) Intracellular zinc levels in the long-term Jurkat T cell model measured after three weeks either with FluoZin-3 AM (E, n = 18) or Zinpyr-1 (F, n = 17) by flow cytometry.

(G, H and I) IL-2 was analyzed by ELISA in the supernatants of HuT-78 (G, n = 3) and Jurkat (H, n = 6) T cells stimulated for 24 h with a combination of phorbol-12-myristate-13-acetate (PMA, 10 ng/mL) and calcimycin (Cal, 0.1 µM) in the short-term model and in Jurkat T cells after long-term zinc deficiency and PMA/Cal or phytohemagglutinin (PHA, 2.5 µg/mL) stimulation (I, n = 19).

(J and K) IL-2 expression in Jurkat T cells after long-term zinc deficiency stimulated for 6 h (J, n = 12) or 24 h (K, n = 12) with PMA/Cal (10 ng/mL/0.1 µM) or PHA (2.5 µg/mL). IL-2 expression was determined on RNA level by qPCR using PBGD as housekeeping gene. Expression levels were normalized to untreated Jurkat control cells.

Data information: Data are shown as mean + SEM from independent experiments. *P<0.05, **P<0.01, ***P<0.001 (Student's t-test).

Fig. 2. Zinc transporter expression is altered by zinc deficiency (ZnD).

Zip importer (A) and ZnT exporter (B) expression were analyzed in Jurkat T cells by qPCR after three weeks of zinc deficiency compared to control cells. All Zip importers were expressed except Zip12 and all ZnT exporters were expressed except ZnT2 and ZnT10. PBGD was used as housekeeping gene and expression levels were normalized to untreated Jurkat control cells. Data information: Data are shown as mean + SEM from n = 9 independent experiments. ***P<0.001 (Student's t-test).

Fig. 3. CREMα expression is increased in zinc-deficient (ZnD) T cells and decreased after zinc supplementation in porcine PBMC.

(A and B) Analysis of CREMα expression in HuT-78 (A) and Jurkat (B) T cells on RNA levels in unstimulated and PMA/Cal (10 ng/mL/1 µM)-stimulated cells after 6 h in the short-term model (n = 11). CREMα was normalized to the housekeeping gene PBGD.

(C and D) Analysis of CREMα expression on RNA levels in the long-term zinc deficiency model in Jurkat T cells after stimulation with PMA/Cal and PHA (2.5 µg/mL) for 6 h (C) and 24 h (D) in unstimulated cells (n = 12). CREMα was normalized to the housekeeping gene PBGD.

(E and F) Densitometric quantification of CREMα levels, normalized against β-actin (E, n = 5) and one representative Western Blot using CREMα and β-actin antibodies (F).

(G and H) CREMα protein levels were determined in PBMC isolated from whole blood of pigs supplemented with either 0 ppm, 100 ppm or 2500 ppm zinc from zinc oxide (ZnO). Densitometric quantification of CREMα levels of different pigs (n = 5) per group, normalized to β-actin expression (G) and one representative Western Blot using CREMα and β-actin antibodies (H).

Data information: Data are shown as mean + SEM of independent experiments. **P*<0.05, ***P*<0.01 (Student's t-test (A, B, C, D) or unpaired t-test (G)).

Fig. 4. Increased PP2A activity after long-term zinc deficiency

(A) After three weeks of zinc deficiency (ZnD), activity of the alkaline protein phosphatase was measured within Jurkat T cell lysates compared to control cells with *p*-nitrophenyl phosphate as substrate (n = 5).

(B and C) The IC_{50} was assessed by activity measurements of PP2A after zinc supplementation (0 µM, 0.1 µM, 1 µM, 5 µM, 10 µM and 50 µM $ZnSO_4$) normalized to free zinc measured within the reaction buffer by using FluoZin-3. Enzyme assays were performed with purified PP2A using either a standard peptide as substrate (B) or a more physiological Rb peptide (C, n = 3).

(D) After TPEN supplementation to the PP2A assay for 10 and 20 min, enzyme activity was measured compared to a control (n = 3).

Data information: Data are presented as mean + SEM from independent experiments. **P*<0.05 (Student's t-test).

Fig. 5. Possible zinc targets in the upstream IL-2 and CREMα signaling pathways

Jurkat T cells were incubated for three weeks in zinc deficiency (ZnD) and then either stimulated with PMA/Cal (10 ng/mL/0.1 µM) for 6 h or 24 h or left unstimulated and analyzed by Western Blot.

(A) Densitometric quantification of phosphorylated (p-)PKA substrate normalized to β-actin expression (n = 4) and (**B**) a corresponding representative Western Blot.

(C) Densitometric quantification of c-Fos normalized to β-actin expression (n = 3) and (**D**) a corresponding representative Western Blot.

(E) Densitometric quantification of p-NF-κBp65(S276) normalized to β-actin expression (n = 3) and (**F**) a corresponding representative Western Blot.

(G) Densitometric quantification of p-ERK normalized to ERK expression (n = 3) and (**H**) a corresponding representative Western Blot.

(I) Densitometric quantification of p-H3S10 normalized to H3 expression (n = 6) and (**J**) a corresponding representative Western Blot.

(K) Densitometric quantification of acetylated H3K18 normalized to H3 expression (n = 4) and (**L**) a corresponding representative Western Blot.

Data information: Data are presented as mean + SEM from independent experiments.

Fig. 6. MTF-1 silencing does not alter IL-2 production.

(A) *MTF1* gene silencing was performed with MTF-1 Stealth siRNA and Silencer Select negative control No. 1 siRNA as negative control, which were introduced in Jurkat T cells by electroporation. Success of gene silencing was tested by qPCR after stimulation of cells with PHA (2.5 µg/mL) or PMA/Cal (10 ng/mL/0.1 µM) for 24 h post-transfection or cells were left unstimulated as control (n = 5).

(B) IL-2 levels in the supernatants of siRNA-treated cells were determined by ELISA (n = 5). Data are presented as mean + SEM. ***P*<0.01, ****P*<0.001 (Student's t-test).

Fig. 7. Zinc supplementation decreases HDAC1 activity while H3K9 acetylation is decreased in zinc-deficient T cells

(A) After three weeks of zinc deficiency (ZnD), HDAC1 expression is increased on RNA levels. mRNA expression was analyzed by qPCR in zinc-deficient Jurkat T cells compared to control cells. PBGD was used as housekeeping gene and expression levels were normalized to untreated Jurkat control cells (n = 6).

(B) HDAC1 activity was measured after either adding H_2O as control or 50 µM of zinc sulfate ($ZnSO_4$) (n = 3).

(C) The IC_{50} was assessed by activity measurements of HDAC1 after zinc supplementation (0 µM, 0.1 µM, 1 µM, 5 µM, 10 µM and 50 µM $ZnSO_4$) normalized to free zinc measured in the reaction buffer by using FluoZin-3 (n = 3).

(D) Densitometric quantification of H3K9 acetylation was analyzed after three weeks of zinc deficiency in Jurkat T cells compared to control cells using Western Blot and referred to H3 protein expression (n = 3) and **(E)** one representative Western Blot using the indicated acetyl-H3K9 and H3 antibodies.

Data information: Data are presented as mean + SEM from independent experiments. *P<0.05. **P<0.01 (Student's t-test).

Fig. 8. Overview of zinc-affected molecules involved in the upstream IL-2 signaling pathway. Zinc targets identified in T cells in the present study, which are associated to impaired IL-2 expression, are presented. Increased CREMα levels under zinc-deficient conditions are ensured by increased PP2A activity. In detail, higher dephosporylation of SP-1 by PP2A can be assumed, likely leading to enhanced SP-1 binding to the CREM promoter. Subsequently, due to the increased CREMα expression, IL-2 transcription is reduced by binding to and recruiting HDAC1 to the IL-2 promoter. HDAC1 activity is increased under zinc-deficient conditions, causing increased deacetylation of H3K9. Regulation of zinc homeostasis in zinc-deficient T cells is accompanied by Zip10 upregulation and downregulation of ZnT1, ZnT3 and ZnT8.

Supporting Information

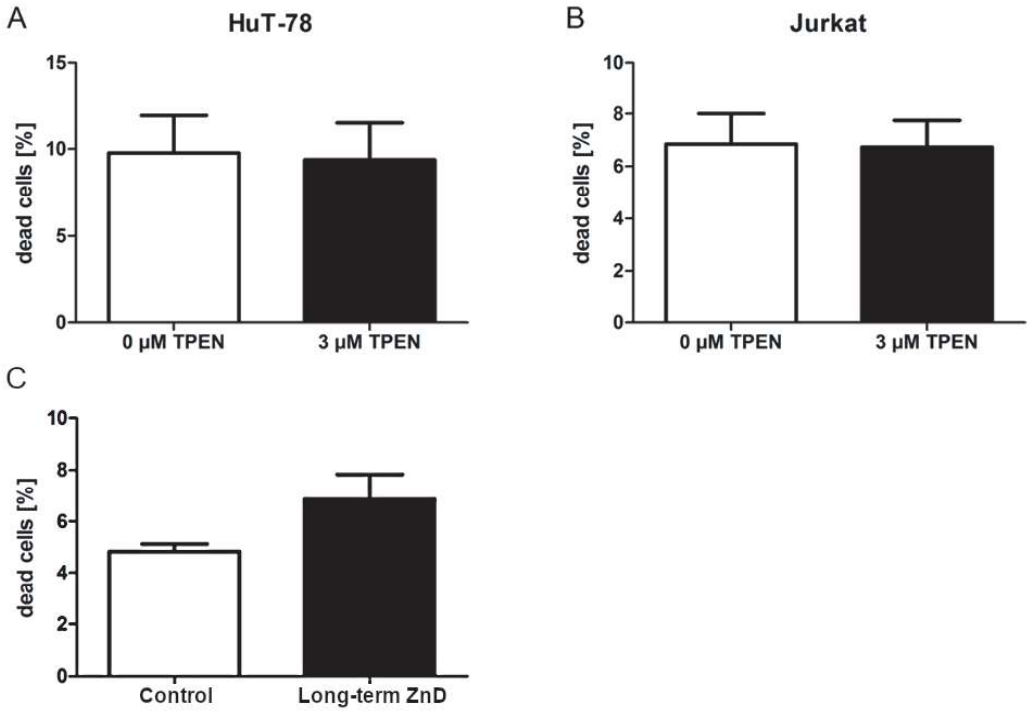

Fig. S1. No toxic effect of TPEN incubation and long-term zinc deficiency.

PI measurements of HuT-78 (A) and Jurkat (B) T cells after three days incubation with 3 µM TPEN compared to cells, which were incubated without TPEN (n = 4). (C) PI measurement of Jurkat T cells after three weeks incubation in Chelex-treated and pH-adjusted (7.4) medium supplemented with minimal amounts of $ZnSO_4$ (0.174 µM) (n = 19). Measurements were performed by flow cytometry. Data are shown as mean + SEM from independent experiments. No significant differences were determined by using Student's t-test.

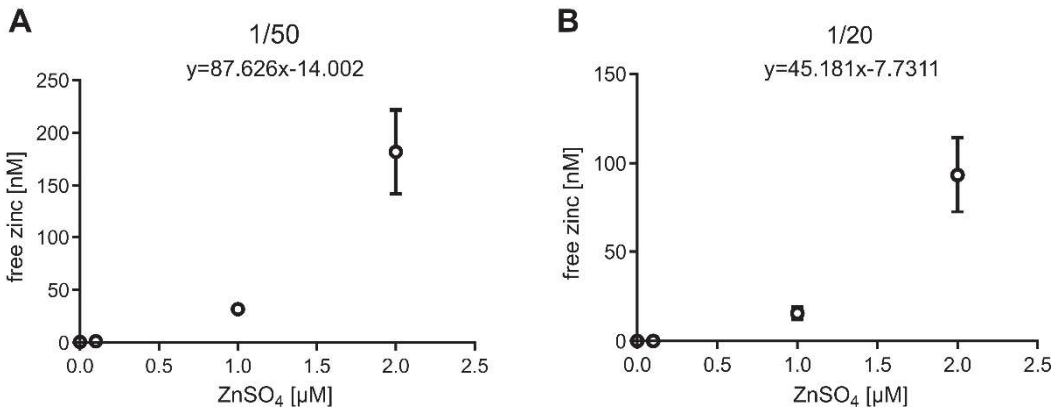

Fig. S2. Determination of the amount of free zinc within the PP2A buffer.

After supplementing $ZnSO_4$ (0 µM, 0.1 µM, 1 µM and 2 µM) to the PP2A buffer, the free zinc concentration within the buffer was measured by Fluozin-3 tetrapotassium salt at the fluorescence plate reader Spark. (A) One 1/50 dilution of PP2A preparation was used within the assay on a standard peptide. Due to the concentration optimum of FluoZin-3, measurement of free zinc at higher supplemented zinc concentrations was not possible. Assuming linear dependency, the formula y = 87.626x - 14.002 is generated, which can be used for calculation of free zinc at higher supplemented zinc concentrations. (B) One 1/20 dilution of PP2A preparation was used within the assay on the more physiological Rb peptide. Assuming linear dependency, the formula y = 45.181x - 7.7311 is generated, which can be used for calculation of free zinc at higher supplemented zinc concentrations. Data are shown as mean ± SEM from n=3 independent experiments.

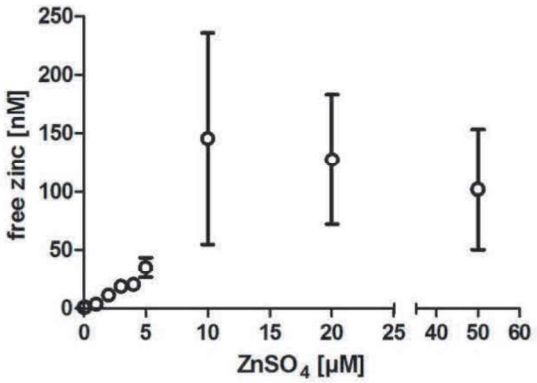

Fig. S3. Determination of the amount of free zinc within the HDAC1 buffer.

After supplementing $ZnSO_4$ (0 µM, 0.1 µM, 1 µM, 2 µM, 3 µM, 4 µM, 5 µM, 10 µM, 20 µM and 50 µM) to the HDAC1 buffer, the free zinc concentration within the buffer was measured by Fluozin-3 tetrapotassium salt at the fluorescence plate reader Ultra 384. Data are shown as mean ± SEM from n=3 independent experiments.

Table S1. Porcine serum zinc is increased after zinc supplementation.

Shown are means and standard error of the mean (SEM) for each zinc-supplemented pig group (0 ppm, 100 ppm and 2500 ppm) with n=5-6. Significant changes are indicated (** $p<0.01$; unpaired t-test).

zinc group		zinc [µg/dl]
0 ppm	mean	52.42
	SEM	5.19
100 ppm	mean	55.09
	SEM	2.32
2500 ppm	mean	107.11 †
	SEM	14.76

† significant compared to 0 ppm (**) and 100 ppm (**) zinc-supplemented pigs

Table S2. Zinc supplementation increases IL-2 production of porcine PBMC.

Isolated PBMC were either left unstimulated as control or were stimulated with a combination of PMA (10 ng/ml) and Calcimycin (Cal, 0.1 µM) to induce IL-2 production. Means and SEM from n=5 pigs are shown. Significant changes are indicated (** p<0.01, *** p<0.001; unpaired t-test).

zinc group		control [pg/ml]	PMA/Cal [pg/ml]
0 ppm	mean	26.04	2638.72
	SEM	3.49	371.87
100 ppm	mean	24.53	2299.78
	SEM	2.46	180.13
2500 ppm	mean	32.06	4653.56 †
	SEM	3.53	191.29

† significant compared to 0 ppm (**) and 100 ppm (***) zinc-supplemented pig

Table S3. Extract of the data set obtained after methylation pattern analysis.

Shown are the raw data obtained after methylation analysis using an EPIC BeadChip Microarray. DNA methylation was analyzed in Jurkat T cells either cultured for three weeks in control medium (control) or in zinc-deficient medium (ZnD) with n=6. Moderated t-statistics were calculated with the eBayes function from the limma package.

CpG_loci_identifier	**cg17850932**
ProbeID_A	4763177
ProbeID_B	4763177
control_.n1._AVG_Beta	0,7137833
control_.n2._AVG_Beta	0,6063769
control_.n3._AVG_Beta	0,6290151
control_.n4._AVG_Beta	0,5873181
control_.n5._AVG_Beta	0,6391251
control_.n6._AVG_Beta	0,6517482
ZnD_.n1._AVG_Beta	0,6413481
ZnD_.n2._AVG_Beta	0,5687808
ZnD_.n3._AVG_Beta	0,6304657
ZnD_.n4._AVG_Beta	0,6135375
ZnD_.n5._AVG_Beta	0,5441108
ZnD_.n6._AVG_Beta	0,6248515
Chromosome	4
MAPINFO	123377900
logFC †	-0,0340454
AveExpr ‡	0,62087176
Moderated t-Statistic	-1,5882464
P-Value	0,13667216
Adjusted P-Value	0,86217449
B §	-5,8558272

† estimate of the log2-fold-change between the two conditions

‡ average log2-expression for the probe over all arrays and channels

§ log-odds that the gene is differentially expressed

Figure 1

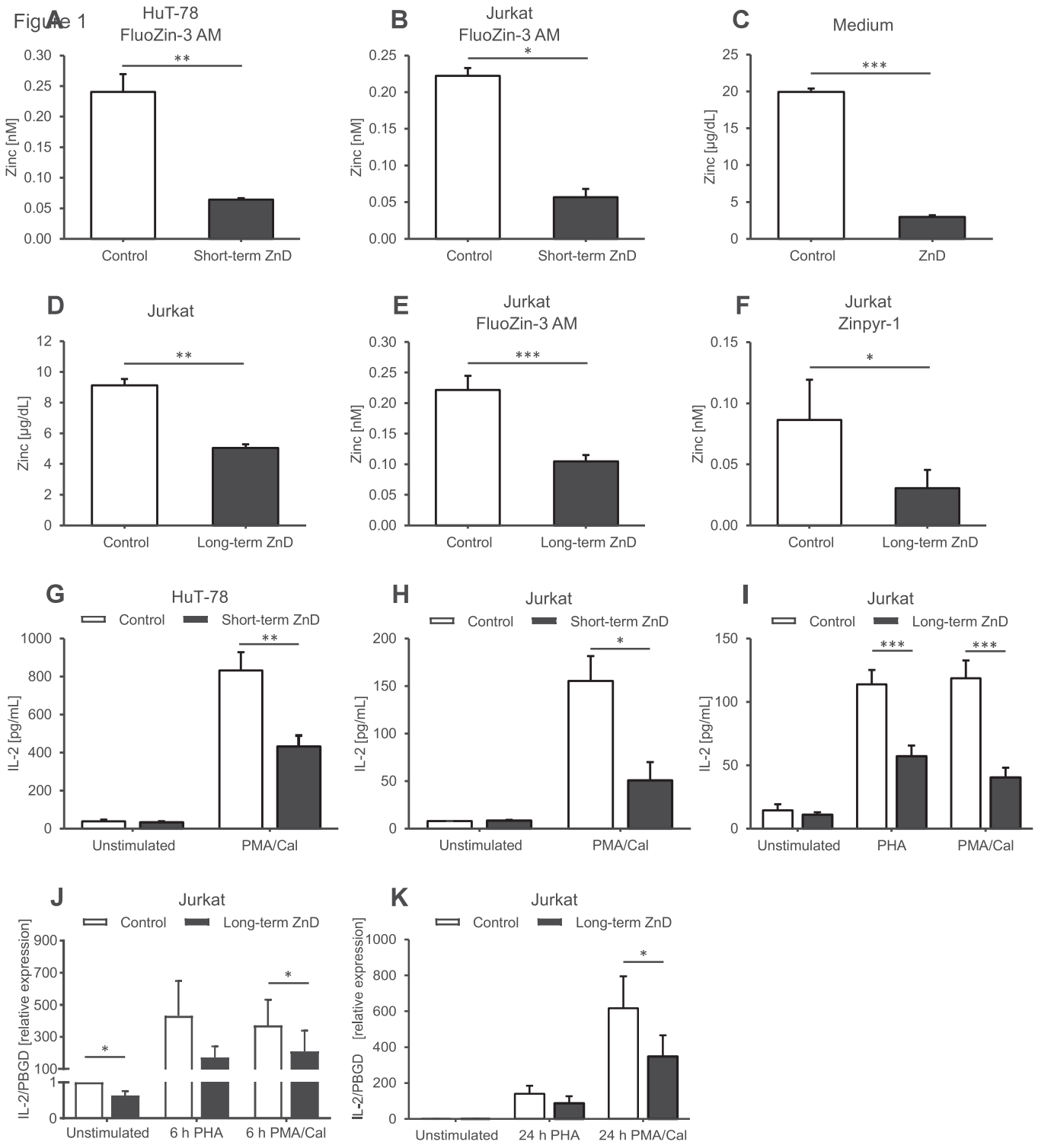
A
HuT-78
FluoZin-3 AM
Zinc [nM]
Control
Short-term ZnD
B
Jurkat
FluoZin-3 AM
Zinc [nM]
Control
Short-term ZnD
C
Medium
Zinc [µg/dL]
Control
ZnD
D
Jurkat
Zinc [µg/dL]
Control
Long-term ZnD
E
Jurkat
FluoZin-3 AM
Zinc [nM]
Control
Long-term ZnD
F
Jurkat
Zinpyr-1
Zinc [nM]
Control
Long-term ZnD
G
HuT-78
Control
Short-term ZnD
IL-2 [pg/mL]
Unstimulated
PMA/Cal
H
Jurkat
Control
Short-term ZnD
IL-2 [pg/mL]
Unstimulated
PMA/Cal
I
Jurkat
Control
Long-term ZnD
IL-2 [pg/mL]
Unstimulated
PHA
PMA/Cal
J
Jurkat
Control
Long-term ZnD
IL-2/PBGD [relative expression]
Unstimulated
6 h PHA
6 h PMA/Cal
K
Jurkat
Control
Long-term ZnD
IL-2/PBGD [relative expression]
Unstimulated
24 h PHA
24 h PMA/Cal

Figure 2

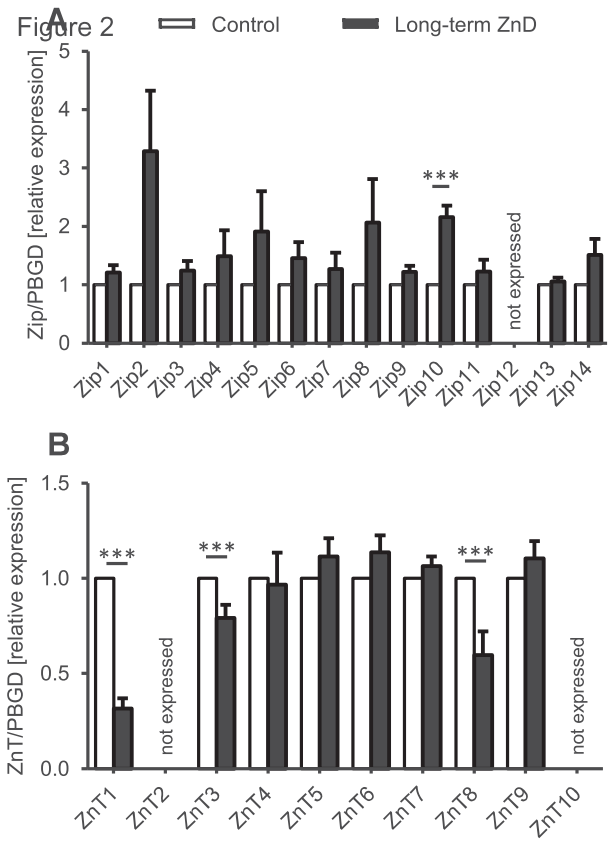
A
Control
Long-term ZnD
Zip/PBGD [relative expression]
0
1
2
3
4
5
***
not expressed
Zip1
Zip2
Zip3
Zip4
Zip5
Zip6
Zip7
Zip8
Zip9
Zip10
Zip11
Zip12
Zip13
Zip14
B
ZnT/PBGD [relative expression]
0.0
0.5
1.0
1.5
***
***
***
not expressed
not expressed
ZnT1
ZnT2
ZnT3
ZnT4
ZnT5
ZnT6
ZnT7
ZnT8
ZnT9
ZnT10

Figure 3

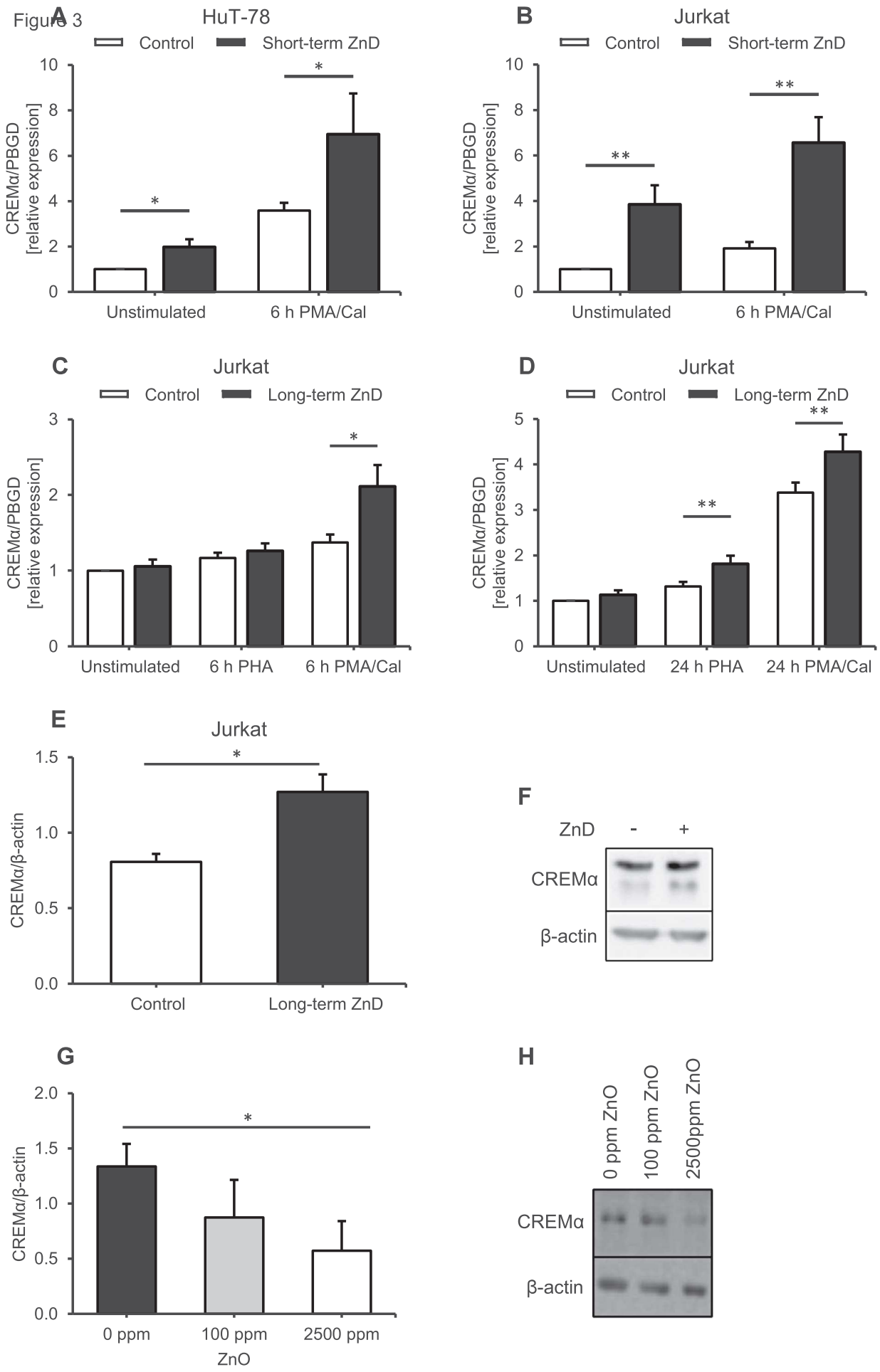
A
HuT-78
Control
Short-term ZnD
CREMα/PBGD [relative expression]
Unstimulated
6 h PMA/Cal
B
Jurkat
Control
Short-term ZnD
CREMα/PBGD [relative expression]
Unstimulated
6 h PMA/Cal
C
Jurkat
Control
Long-term ZnD
CREMα/PBGD [relative expression]
Unstimulated
6 h PHA
6 h PMA/Cal
D
Jurkat
Control
Long-term ZnD
CREMα/PBGD [relative expression]
Unstimulated
24 h PHA
24 h PMA/Cal
E
Jurkat
CREMα/β-actin
Control
Long-term ZnD
F
ZnD
-
+
CREMα
β-actin
G
CREMα/β-actin
0 ppm
100 ppm
2500 ppm
ZnO
H
0 ppm ZnO
100 ppm ZnO
2500ppm ZnO
CREMα
β-actin

Figure 4

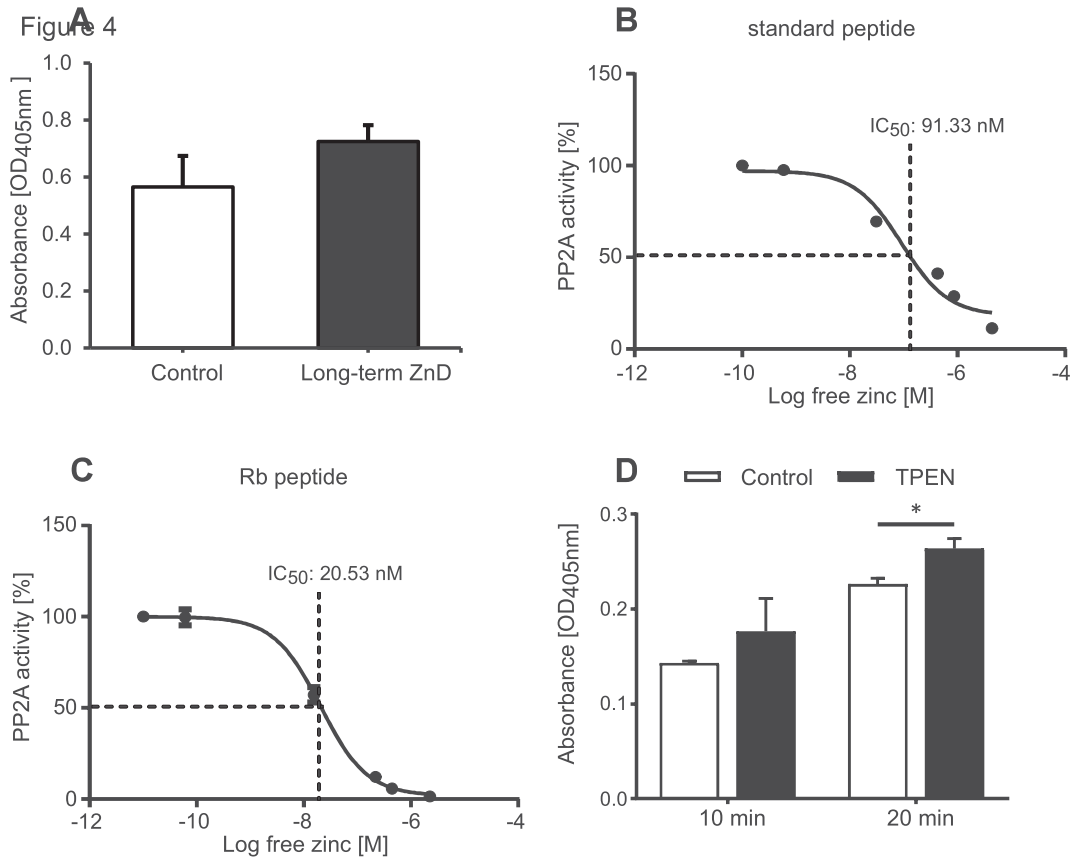
A
Absorbance [OD405nm]
1.0
0.8
0.6
0.4
0.2
0.0
Control
Long-term ZnD
B
standard peptide
PP2A activity [%]
150
100
50
0
IC50: 91.33 nM
-12
-10
-8
-6
-4
Log free zinc [M]
C
Rb peptide
PP2A activity [%]
150
100
50
0
IC50: 20.53 nM
-12
-10
-8
-6
-4
Log free zinc [M]
D
Control
TPEN
*
Absorbance [OD405nm]
0.3
0.2
0.1
0.0
10 min
20 min

Figure 5

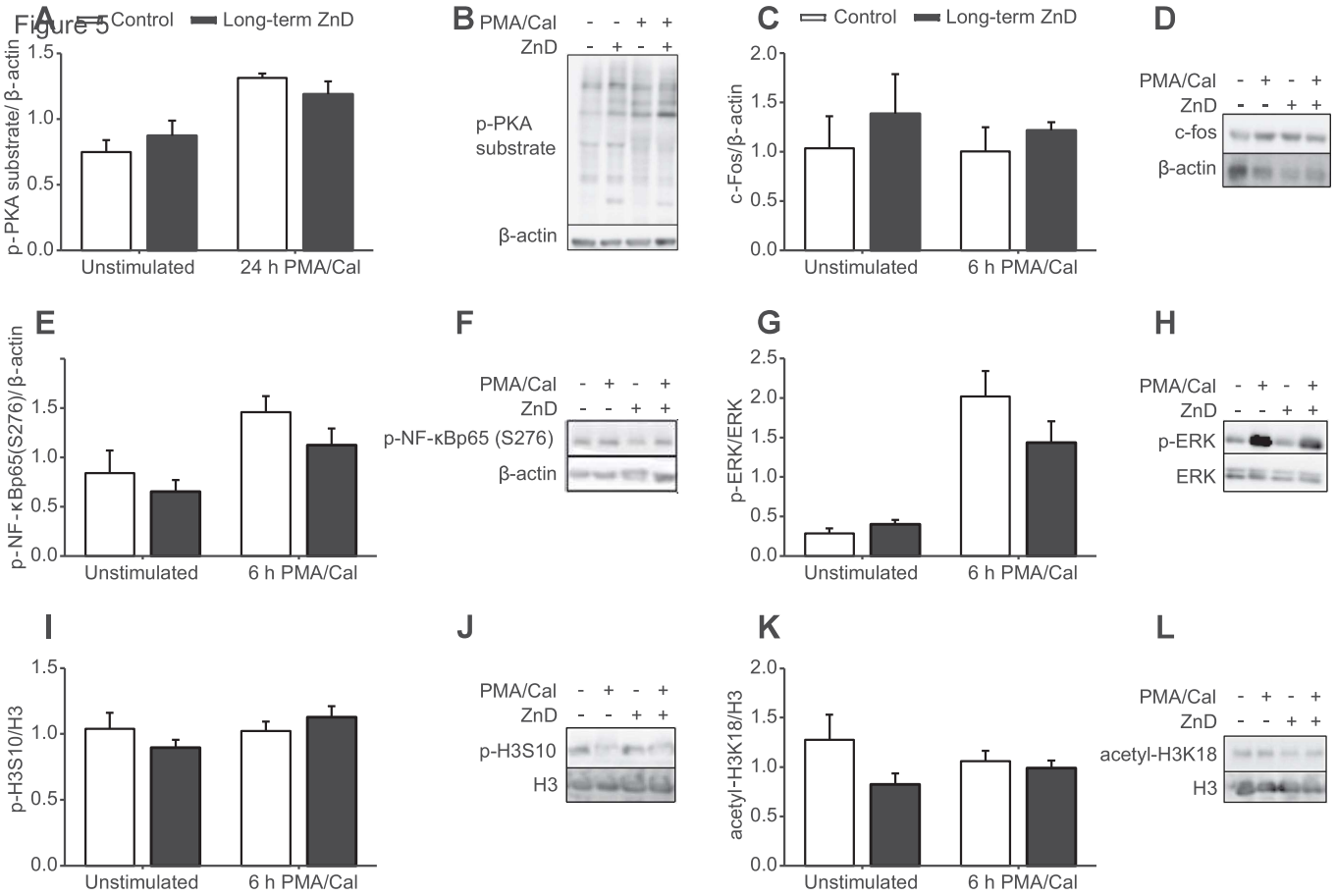
A
Control
Long-term ZnD
p-PKA substrate/β-actin
1.5
1.0
0.5
0.0
Unstimulated
24 h PMA/Cal
B
PMA/Cal - - + +
ZnD - + - +
p-PKA substrate
β-actin
C
Control
Long-term ZnD
c-Fos/β-actin
2.0
1.5
1.0
0.5
0.0
Unstimulated
6 h PMA/Cal
D
PMA/Cal - + - +
ZnD - - + +
c-fos
β-actin
E
p-NF-κBp65(S276)/β-actin
1.5
1.0
0.5
0.0
Unstimulated
6 h PMA/Cal
F
PMA/Cal - + - +
ZnD - - + +
p-NF-κBp65 (S276)
β-actin
G
p-ERK/ERK
2.5
2.0
1.5
1.0
0.5
0.0
Unstimulated
6 h PMA/Cal
H
PMA/Cal - + - +
ZnD - - + +
p-ERK
ERK
I
p-H3S10/H3
1.5
1.0
0.5
0.0
Unstimulated
6 h PMA/Cal
J
PMA/Cal - + - +
ZnD - - + +
p-H3S10
H3
K
acetyl-H3K18/H3
2.0
1.5
1.0
0.5
0.0
Unstimulated
6 h PMA/Cal
L
PMA/Cal - + - +
ZnD - - + +
acetyl-H3K18
H3

Figure 6

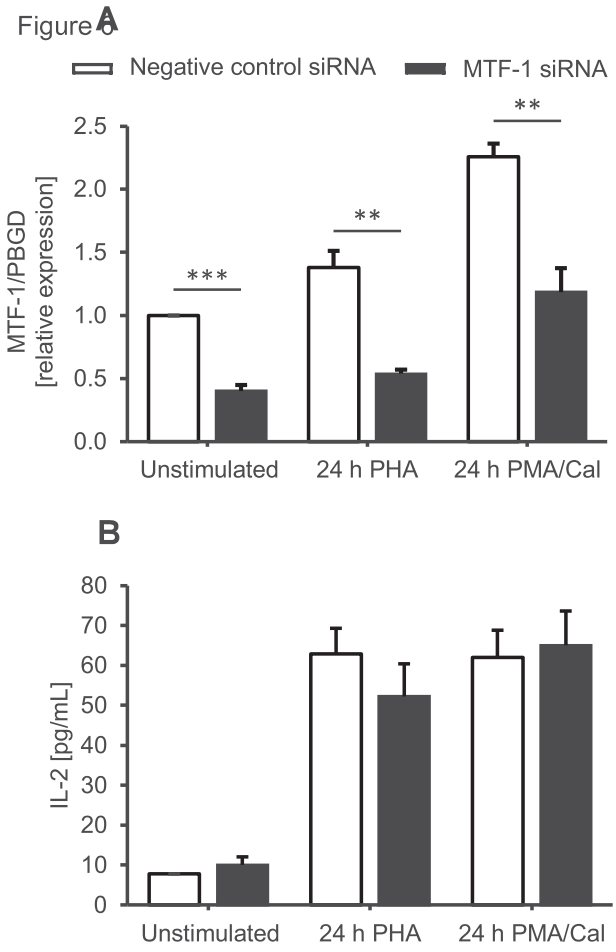
A
Negative control siRNA
MTF-1 siRNA
MTF-1/PBGD [relative expression]
2.5
2.0
1.5
1.0
0.5
0.0
***
**
**
Unstimulated
24 h PHA
24 h PMA/Cal
B
IL-2 [pg/mL]
80
70
60
50
40
30
20
10
0
Unstimulated
24 h PHA
24 h PMA/Cal

Figure 7

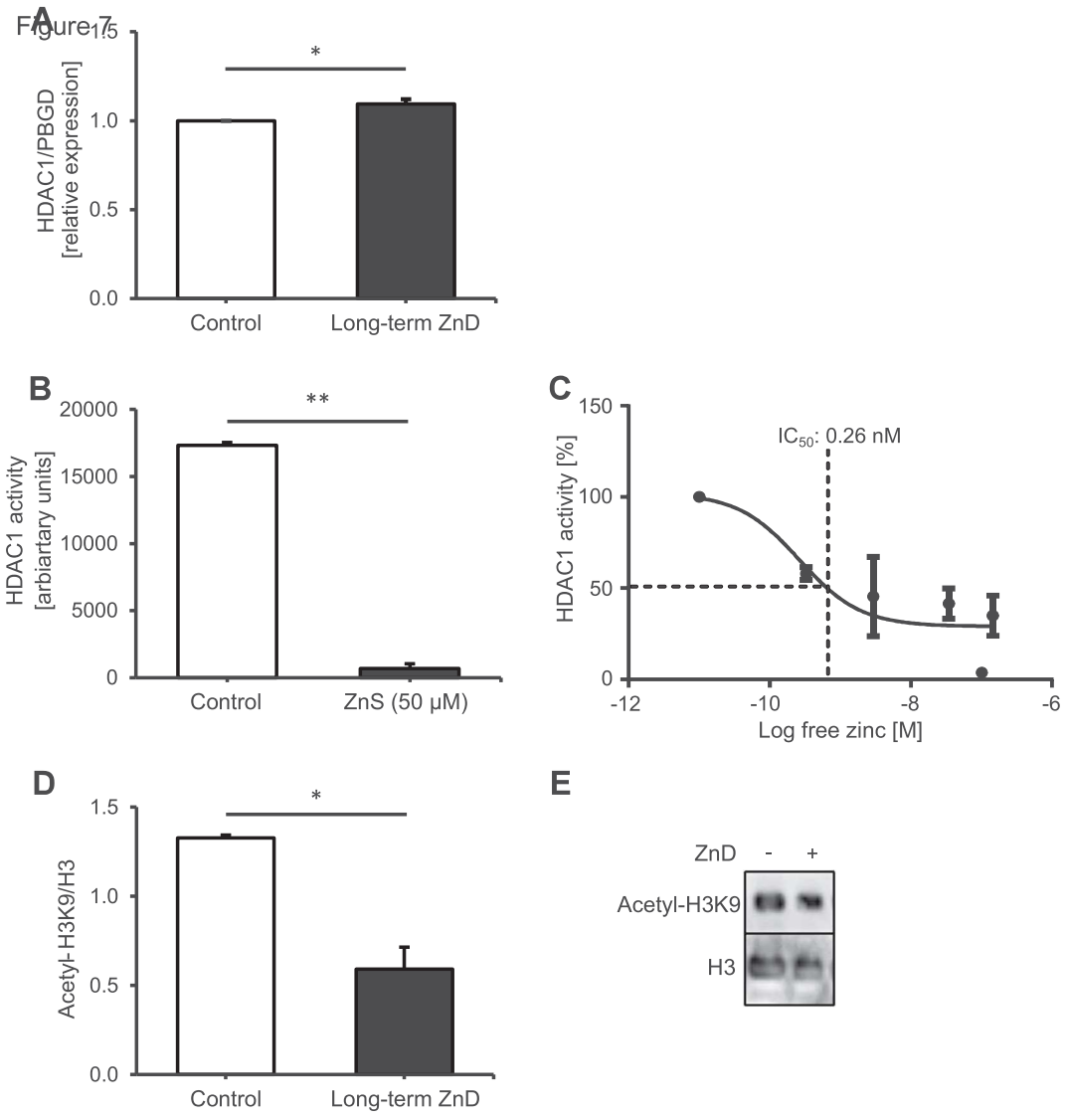
A
HDAC1/PBGD [relative expression]
1.5
1.0
0.5
0.0
*
Control
Long-term ZnD
B
HDAC1 activity [arbiartary units]
20000
15000
10000
5000
0
**
Control
ZnS (50 μM)
C
HDAC1 activity [%]
150
100
50
0
IC50: 0.26 nM
-12
-10
-8
-6
Log free zinc [M]
D
Acetyl-H3K9/H3
1.5
1.0
0.5
0.0
*
Control
Long-term ZnD
E
ZnD - +
Acetyl-H3K9
H3

Figure 8

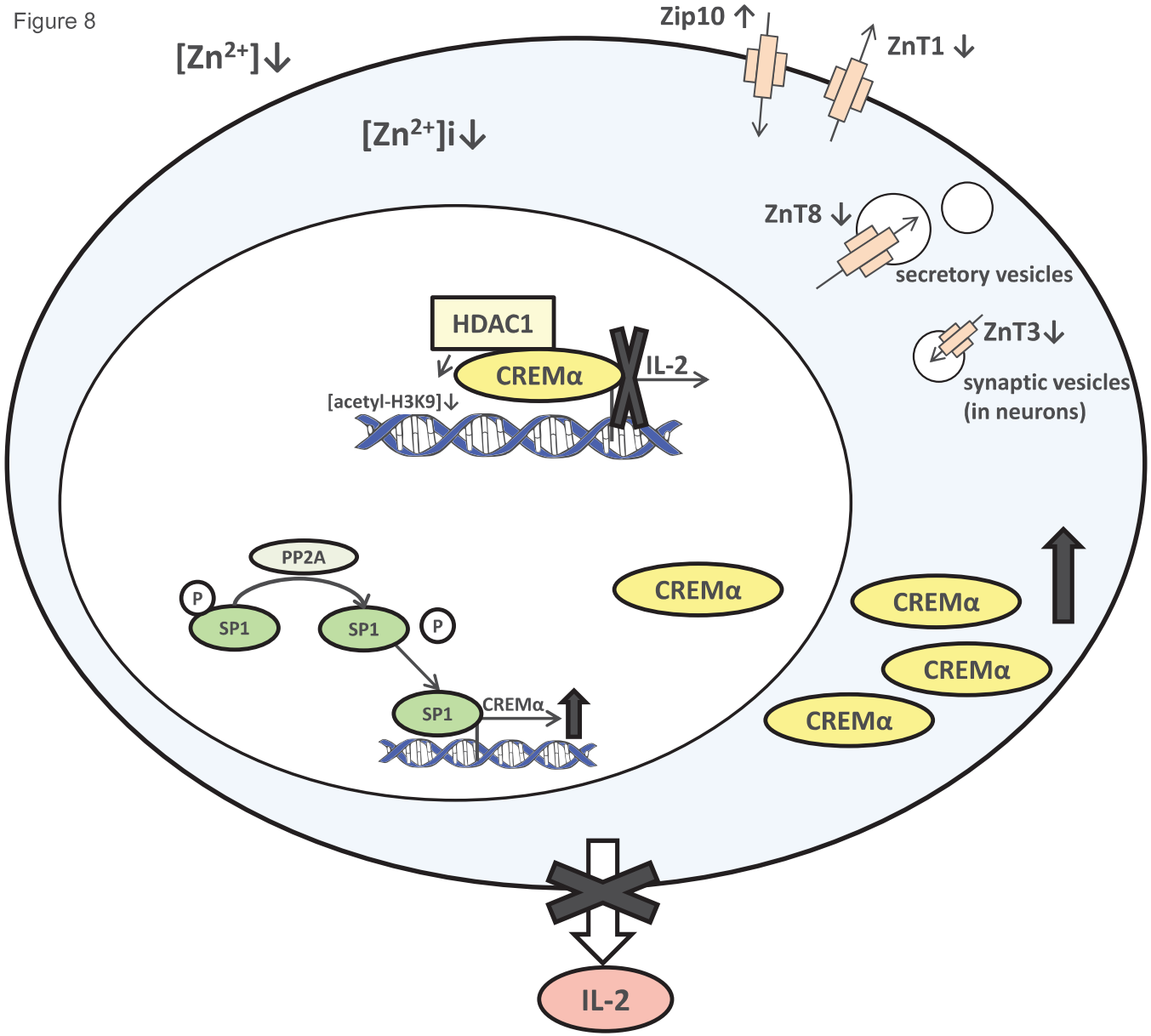
[Zn2+]↓
[Zn2+]i↓
Zip10 ↑
ZnT1 ↓
ZnT8 ↓
secretory vesicles
ZnT3↓
synaptic vesicles
(in neurons)
HDAC1
CREMα
IL-2
[acetyl-H3K9]↓
PP2A
P
SP1
SP1
P
SP1
CREMα
CREMα
CREMα
CREMα
CREMα
IL-2